BMR RESEARCH NEWSLETTER

'Geoscience for Australia's Future'

Number 16 April 1992

In this issue:

Au–Pt–Pd–U mineralisation in the Coronation Hill–El Sherana region, NT.

In 1990, BMR's Minerals and Land Use Program was awarded a contract by the Resource Assessment Commission (RAC) Inquiry into the Kakadu Conservation Zone to 'conduct and interpret geological, geochemical and geophysical surveys as required to provide the best possible basis, within the limited time available, for estimating the resource potential in the Conservation Zone'. All company data for the Conservation Zone were reviewed and further stream-sediment, soil, and rock-chip geochemical surveys were undertaken. The resource potential of 50 of the 57 known prospects, mines and mineral occurrences was then assessed on the basis of this and earlier work (Fig. 1 shows localities visited). Although several distinct styles of mineralisation are present, systematic variations in structural settings, rock alteration characteristics, and rock types suggest that all mineralisation is related to one event. There is a rock-controlled distinction between the styles of mineralisation present at or near the unconformity, with Au and Pd/Pt more common in feldspar-bearing rocks; U (± Au ± Pt/Pd) is usually only found in either carbon-rich shales or chloritic rocks. The mineral deposits are surrounded by altered rocks that are depleted in Na, Ca, Si, and Th. These same elements have been moved to higher structural levels above the unconformity, where quartz veins can have Au associated with minor amounts of As, Cu and/or U, but not Pt or Pd; at even structurally higher levels, zones of Th and P_2O_5-enrichment are found. These element associations may be indicators of Au, Pt, Pd, and U mineralisation at depth. A far greater proportion of the Coronation Hill deposit is hosted by the pre-1870 Ma sequence than was previously thought, and the distinction between the metal styles at El Sherana and Coronation Hill is related to stratigraphic position.

Further insights into metallogenic controls

The new surveys have allowed refinement of the existing metallogenic model, and identified several important new controls on the style and types of metal concentrations, which may assist in exploration for unconformity-related Au ± Pt ± Pd ± U deposits. Three characteristics of the mineralisation in the Coronation Hill–El Sherana Region have already been noted (*BMR Research Newsletter,* 12, 1990): (1) all known mineralisation lies close to the unconformity between the Coronation Sandstone (El Sherana Group) and pre-1870 Ma basement sequences; (2) most is on or near the Rockhole–Palette Fault System (Fig. 1); and (3) all deposits are surrounded by alteration zones, which in places extend over 1 km from the mineralisation.

Two new important observations from the 1990 field program are related to stratigraphic position and variation in metal content.

Regional stratigraphic position

Carville & others (1991: *World Gold 91*, 287–293) correlated the diorite at Coronation Hill with the Zamu Dolerite, arguing that most of the porphyries in the ore zone are older than the 1870 Ma unconformity and not part of the 1860 Ma El Sherana Group, as previously considered. We now correlate the 'green tuffaceous shale unit', also an important host to mineralisation at Coronation Hill, with the Shovel Billabong Andesite of the Kapalga Formation. The relative stratigraphic position of Coronation Hill and El Sherana deposits is shown in Figure 2. The main difference is that Coronation Hill is higher than El Sherana, which is predominantly hosted by carbonaceous shales of the Koolpin Formation.

Variation in metal content in mines and prospects

The rock-chip geochemical data from prospects and mines of the Coronation Hill–

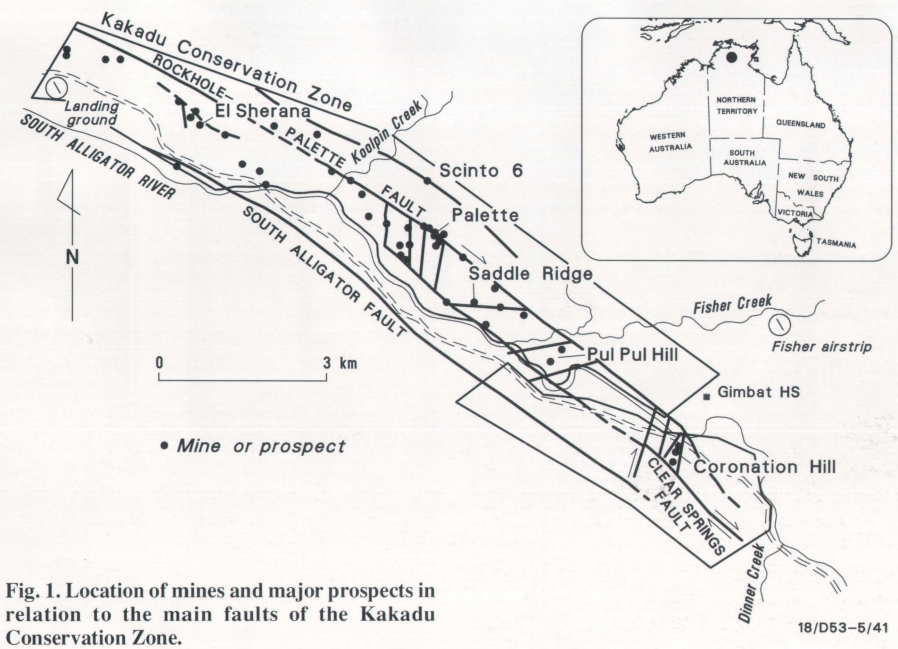

Fig. 1. Location of mines and major prospects in relation to the main faults of the Kakadu Conservation Zone.

BMR GEOLOGY AND GEOPHYSICS AUSTRALIA

Bureau of Mineral Resources, Geology & Geophysics

a research bureau of the Department of Primary Industries and Energy

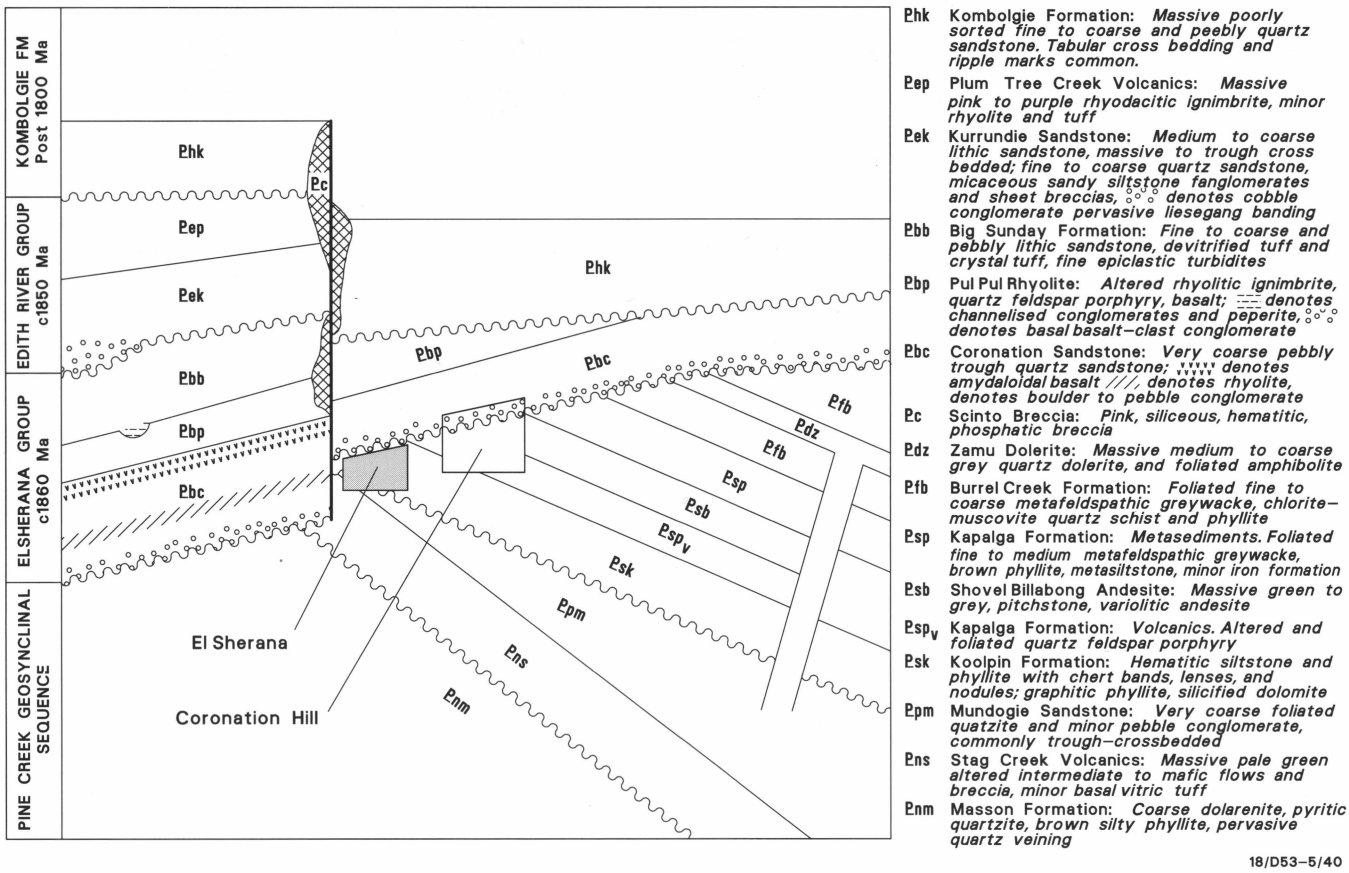

Fig. 2. Schematic rock relationship diagram and brief geological description of rock units of the Coronation Hill–El Sherana Region (based on Friedman, 1991, *op. cit.*). Boxes show stratigraphic setting of Coronation Hill and El Sherana deposits.

El Sherana region, together with company information, show several different metal associations, apparently related to both host-rock composition and vertical distance above or below the unconformity. These associations are:

(a) Au–Pt–Pd or U–Au–Pt–Pd at or near the unconformity. The presence or absence of U in the Au–Pt–Pd mineralisation appears related to geological differences (summarised in Table 1), primarily in host-rock composition. U-bearing deposits are hosted mainly in carbonaceous shales, although some U is associated with chloritic zones. Deposits lacking U, best developed at Coronation Hill, occur in a broad range of host rocks, including quartz–feldspar porphyry, green tuffaceous shale, diorite, dolomite, and sedimentary breccias. Although seemingly diverse rock types, the common components of these U-poor host units are feldspar and/or carbonate.

(b) Au hosted by cherty ferruginous shale below the unconformity. This association contains Au ± Cu ± Ag with only rare U; and is only found below the unconformity in cherty ferruginous shale of the Koolpin Formation, particularly where it is in contact with carbonaceous shale, which commonly also contains U mineralisation.

(c) Au ± As ± Cu (without either Pt or Pd) associated with quartz veins above the unconformity. This quartz vein deposit is always found above the unconformity, generally hosted by the Coronation Sandstone.

An integrated model

Combining the old and new data, an integrated model for the deposit types can now be developed. Although differing in metal content, all mines and prospects of the Coronation Hill region share similar timing and structural controls, suggesting that they are related to one geochemical system. Detailed studies (reported elsewhere in this issue) have shown that both U-rich and U-poor Au—Pt—Pd mineralisation were formed by descending, low-temperature, highly oxidised, very saline, meteoric fluids. The segregation of U was controlled by fluid—rock interaction in the feldspathic or carbonate rocks. Interaction caused an increase in pH, thus precipitating

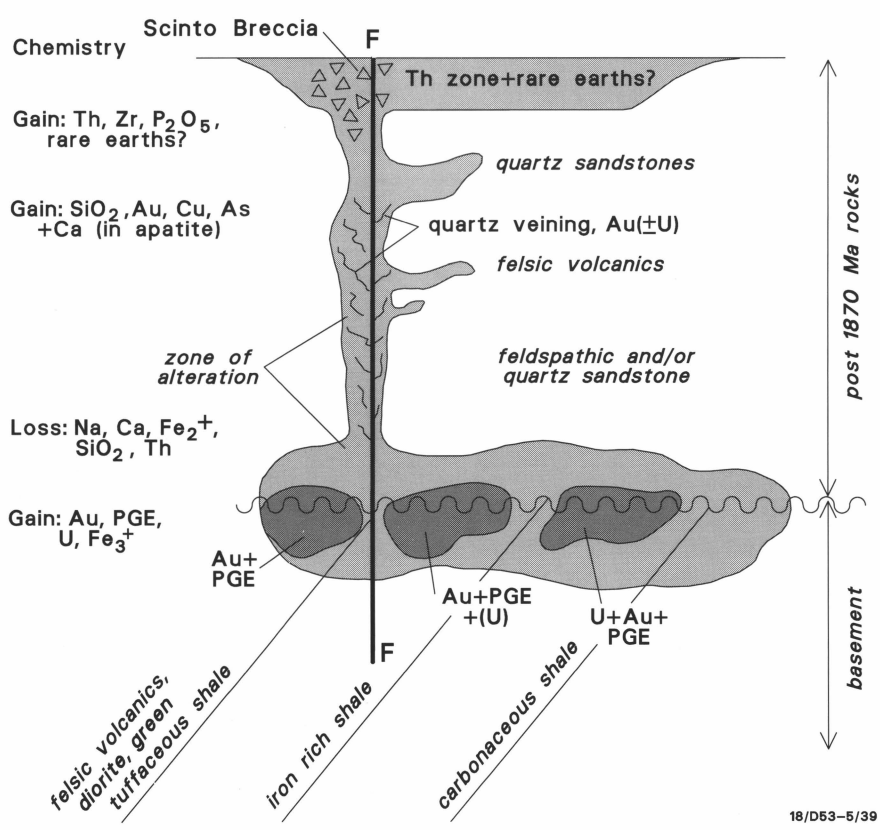

Fig. 3. Model of possible relationship between different styles of mineralisation in the Coronation Hill–El Sherana Region.

Au, Pt, Pd, but not U. However, interaction with carbonaceous or chloritic rocks resulted in a reduction in fO_2, and consequent precipitation of U, Au, Pt and Pd. The other two types of metal associations can be explained by further reaction of the mineralising fluids.

Desilicification is common in the Au–Pt–Pd ± U mineralisation close to the unconformity. It is therefore possible that the quartz vein or silicification zones, prevalent in prospects above the unconformity, may overlie structurally deeper desilicified and potentially mineralised zones (Fig. 3).

Only highly oxidised fluids can carry U, Au, Pt, and Pd together in solution (e.g. Wilde & others, 1989: *Economic Geology, Monograph* 6, 637–650). When such fluids interacted with the carbonaceous and, sometimes, sulphide-bearing parts of the basement sequence, most of the U, Au, Pt, and Pd would have been precipitated. In the more sulphide-rich parts of the basement, fluids could have become more chemically reducing and hence capable of transporting Au, As, Cu and Ag. These elements then were probably precipitated either at higher structural levels in association with quartz (Fig. 3) or, in the case of the El Sherana deposit, in cherty ferruginous shales adjacent to carbonaceous shales.

Another possible indicator of ore localisation is the Scinto Breccia, shown by Friedman (1991, *BMR Record* 1991/108) to be partly related to the same major fault zones that controlled mineralisation. The Scinto Breccia is commonly enriched in P_2O_5 (up to 17 wt%), with consistently high values (up to 5 wt% P_2O_5) in some deposits, particularly, as shown by the rock-chip survey, in the Cliff Face–Palette–Skull area. Thus, outcrops of the fault-associated P_2O_5-rich Scinto Breccia may indicate mineralisation at depth.

Depletion of Th in the alteration zones around the deposits implies that Th must have been precipitated elsewhere: zones of Th-enrichment are known close to major fault systems, e.g. at El Sherana and Pul Pul Hill. Th-enrichment may, therefore, indicate buried unconformity-related mineralisation (Fig. 3).

Conclusion

The different metallogenic types in the Coronation Hill–El Sherana region are related to one fluid system: Au–Pt–Pd ± U precipitating as meteoric fluids descended and intersected the unconformity; on the upward or outward path SiO_2, P_2O_5, Au, Cu and Ag were deposited. For other areas, outside the Kakadu region, Au–Pt–Pd mineralisation without U appears to have been controlled by feldspar-bearing rocks, below or at the unconformity, with only minor carbonaceous and/or chloritic material. In regions with potential for this style of mineralisation, zones of silicification, P_2O_5-enrichment, or Th-enrichment, along major fault structures, may indicate unconformity-type Au ± Pt ± Pd ± U mineralisation at depth.

For further information, contact Dr Lesley Wyborn (Minerals and Land Use Program) at BMR.

Parameter	Au–Pd–Pt	U–Au–Pd–Pt
Host rocks	Quartz–feldspar porphyry, green tuffaceous siltstone, diorite, siliceous dolomite, sedimentary breccia, cherty iron-rich shale	Carbonaceous shale, cherty ferruginous shale, quartz–feldspar porphyry
Stratigraphic setting	More common in dolomitic/volcanic basement rocks, intruded by quartz–feldspar porphyry	More commonly associated with Koolpin Formation
Structural setting	Fracture zone associated with the Rockhole–Palette Fault	Fracture zones associated with the Rockhole–Palette Fault
Mineralisation style	Quartz–carbonate–chlorite veins, often with chloritic alteration	Pitchblende veins ± chlorite–white mica alteration; quartz absent
Alteration	Minor chlorite, sulphide silicification	Desilicification, chloritisation
Timing	Post Kombolgie Formation	Post Kombolgie Formation
Structural control	(a) Fractures distributed on north-trending fault offsets or bends (b) Unconformity	(a) Fault bend/intersections (b) Unconformity (c) Competency contrast between cherty ferruginous shale and carbonaceous shale
Possible precipitation mechanisms	(a) Reduction of oxidised fluids by interaction with chloritic rock types (b) Titration of slightly acidic metal-bearing fluids to high pH by interaction of fluid and calcareous or K-bearing rock types	(a) Reduction of oxidised fluids from above unconformity by interaction with carbonaceous rocks below unconformity (b) Mixing of oxidised fluids carrying U–Au–PGE and CH_4-rich fluids (c) Mixing of saline oxidised metal-bearing fluids and low-salinity meteoric or metamorphic fluids

Table 1. Parameters of U-free and U-bearing Au-Pt-Pd mineralisation in the Coronation Hill–El Sherana region (based on Valenta, 1991: *BMR Record* 1991/107)

Fluid inclusion and oxygen-isotope evidence for low-temperature Au–Pt–Pd(± U) mineralisation at Coronation Hill, NT

The Au–Pt–Pd mineralisation (with very low U) at Coronation Hill sets this deposit apart from others in the Pine Creek Geosyncline. Two broad categories of ore mineralogy have been recognised – Au-Platinum Group Elements (PGE) and U–Au–PGE (Carville & others 1990: *in* Hughes, F.E. (Ed), *Geology of the Mineral Deposits of Australia and Papua New Guinea*, pp 759–762), and, although the structural controls are similar to those observed elsewhere in the South Alligator Valley (Wyborn, 1990: *BMR Research Newsletter*, 12), these two types of mineralisation appear to have required different precipitation reactions.

Fluid inclusion data show that this deposit is unlike typical epithermal systems. The initially highly oxidised ore-forming brines descended down near-vertical faults into the Early Proterozoic rocks below the unconformity. Au-PGE precipitated due to a moderate reduction of the fluids and a decrease in pH to feldspar-buffered values of about 5, whereas U-Au-PGE mineralisation was due to a more efficient reduction of the oxidised brine by mixing with reduced fluids originating from below the unconformity.

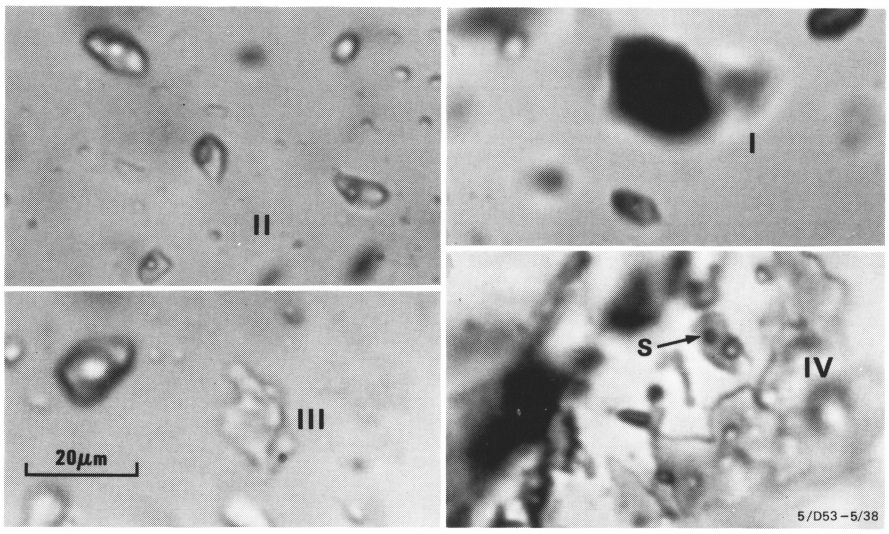

Fig. 4. Photomicrographs showing the nature of fluid inclusions from Coronation Hill. The different types of fluid inclusions are: I, vapor-rich; II, liquid-rich; III, monophase aqueous; and IV, secondary inclusion with a daughter mineral (S).

Fluid inclusions

Fluid inclusions in both types of mineralisation, and in barren veins, fall into four categories (cf. Fig. 4):

Type I inclusions, vapour rich, with 25–100 vol% vapour, are by far the most abundant, and often the only type observed in some microfractures. They are usually irregularly shaped, often with evidence of necking. In many cases, only 100% vapour inclusions were observed in healed microfractures, indicating that a separate vapour phase existed and boiling had occurred.

Type II are two-phase aqueous inclusions with approximately 5 vol% vapour, often coexisting with Type I.

Type III are monophase liquid inclusions, thought to result from the necking down of vapour-rich inclusions.

Type IV are secondary, and generally contain a calcite crystal, an aqueous phase, and less than 10 vol% vapour. Some, however, have up to four solids, including an orange hematite crystal of variable size, probably an accidentally trapped solid.

Types I to III are primary, as they occur together in growth zones in mineralised vein quartz. The two-phase Type II homogenise at approximately 140° C, and the secondary Type IV at around 260° C. The Type IV behave similarly to inclusions in samples collected from other parts of the South Alligator River Valley, indicating the passage of regional fluids associated with earlier alteration events.

The freezing behaviour of the fluid inclusions is complex and was often difficult to observe, owing to most inclusions' small size. Final melting of the primaries ranged from -10 to -55° C, but mostly was close to the ternary eutectic at -52°C in the H_2O–NaCl–$CaCl_2$ system. This shows that the fluids have a high $CaCl_2$ content, as confirmed by Raman spectra of frozen fluid inclusions; both methods gave an average salinity of 26.3 equivalent wt% $CaCl_2$ for the primary fluid. The secondary inclusions generally have salinities below 8 equivalent wt% $CaCl_2$, but a few have intermediate values, suggesting some later stage mixing of high and low salinity fluids.

The laser Raman microprobe did not detect any CO_2, O_2, N2 or CH_4 in the vapour phase of most of the fluid inclusions. However, O_2 was detected in some high-U zones, but is possibly a product of the radiolysis of the trapped water. Several non-ionic solids in Type IV inclusions were also identified during room-temperature Raman studies. The most common daughter minerals were calcite and fine bright orange hematite crystals. A small zone of minor Cu mineralisation also exists at Coronation Hill; its inclusions had either one to three daughter minerals or a mass of clear crystals, some of which were identified by Raman spectroscopy as white mica (most probably sericite). Graphite was also detected in some fluid inclusions from the deeper carbonate veins, indicating a reduced fluid at depth.

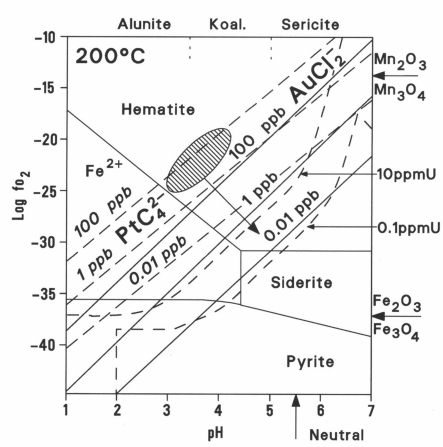

Fig. 5. Log fO_2–pH diagram, showing the distribution of iron phases, and the solubility of U oxides, $AuCl_2^-$, and $PtCl_4^{2-}$ in solution at 200° C. Heavy arrows on the right ordinate mark the position of the hematite + magnetite and Mn_3O_4 + Mn_2O_3 redox buffer assemblages. The hatching indicates the possible pH and oxidation state of the original ore fluid, and the light arrow a possible reaction path.

Oxygen isotope data

The quartz and carbonate veins at Coronation Hill have an average of 13.3‰ O^{18}, varying by± 5‰ O^{18}. The values for the fluid calculated at the average homogenisation temperature of each sample range from -1.7 to -6.6‰ with an average of -3.6‰. The negative $\delta\ ^{18}O$ values of the fluids are incompatible with a magmatic or metamorphic origin, indicating conclusively that meteoric water was the main mineralising fluid.

Mineralisation mechanisms

The fluid inclusion and isotope data constrain the ore genesis models for Coronation Hill. The fluid inclusions demonstrate that the ore fluid was strongly saline with an unusually high $CaCl_2$ content, and that the mineralisation was probably formed from a boiling fluid at around 140° C. Furthermore, the fluids were highly oxidised and the replacement of earlier chlorite by hematite is common throughout the deposit. These characteristics, together with the isotope data show that Coronation Hill is unlike the typical epithermal precious and base-metal deposits, which have completely different element and mineral associations, usually formed at higher temperatures from very low salinity fluids.

Thermodynamic calculations indicate that, under the above conditions, Au and PGE would have been transported as chloride complexes (Fig. 5). The solubility of $AuCl_2$- at 200° C has been calculated by Jaireth (1988: *BMR Record* 1988/9) from the data of Helgeson (1969: *American Journal of Science*, 267, 729–804), and that of $PtCl_4^{2-}$ by thermodynamic interpolation between the low temperature data of Barner & Scheuerman (1978: *Handbook of thermochemical data for compounds of aqueous species, Wiley, New York*, 156p.) and the empirical geothermal data of McKibben & others (1990: *Economic Geology*, 85, 1926–1934). To allow simultaneous comparison of these three chemical systems, the data have been superimposed on the log fO_2 *vs* pH diagram for U, modified from Romberger (1984: *Uranium geochemistry, mineralogy, geology, exploration and resources*, B. de Vivo & others (Eds.), *London Institute of Mining and Metallurgy*, 12–17). The acidic, highly oxidised mineralising fluids originated in conditions as depicted by the hatched field in Figure 5, and descended into the faulted Early Proterozoic Koolpin Formation. Fluid interaction with the feldspathic rocks and periodic boiling initially caused an increase in pH, to buffered values around 5, and a moderate decrease in log fO_2. The above process, shown by the small arrow in Figure 5, could have resulted in the precipitation of significant quantities of Au and PGEs, but most of the uranium would have been kept in solution, thus explaining the Au + PGE mineralisation with little or no U. The fluid inclusion data indicate that the U + Au + PGE mineralisation occurring near the unconformity between the Lower Proterozoic sequence and the overlying capping sandstone resulted from a more efficient reduction of the oxidised brine, probably by mixing with reduced fluids originating from the carbonaceous units below the unconformity.

For further information contact Dr Terry Mernagh at BMR (Minerals and Land Use Program). This work is part of a collaborative project involving the BMR and the partners of the Coronation Hill Joint Venture, who have kindly granted permission to publish this article.

New results from the BMR Yilgarn granite database: implications for metallogeny, tectonics, and lower crustal structure

BMR has compiled a database of some 2700 geochemical analyses from the Yilgarn Craton. The database includes 780 samples of granites and felsic volcanics, most of which were analysed between 1987 and 1989 in collaboration with the Key Centre for Teaching and Research in Strategic Mineral Deposits at the University of Western Australia. The granite data cover the eastern half of the Southern Cross Province and the western part of the Norseman–Wiluna Belt. The prime purpose of the database is to assist geophysical interpretation, particularly seismic and radiometric data. However, on a regional basis, the database is also important to understanding the tectonic and metallogenic evolution, as well as the composition of the lower crust, of the Yilgarn Craton.

In this article, the term 'granite' is used in the broad sense, and incorporates granite, diorite, granodiorite, and tonalite.

Granite geochemistry

On multi-element, primordial mantle-normalised abundance diagrams, four main groups of granites can be recognised:

(1) Early banded gneisses and migmatites: always Sr-undepleted and Y-depleted (Fig. 6A); SiO_2 65–75 wt% , with a distribution peak at 73%. This group was defined by Bettenay (1988: *Geology Department and University Extension Publication* 12, 227–238), and is of minor extent.

(2) Mafic tonalite to granite (*sensu stricto*) suites: Sr-undepleted and Y-depleted in the more mafic end-members, but can become Sr-depleted in the higher SiO_2 end-members (Fig. 1b); SiO_2 48–76 wt% , with a distribution peak at 68%. This group is synonymous with part of the 'internal granites' grouping of Sofoulis (1963: *Geological Survey of Western Australia, Explanatory Notes* SH/15–14). It includes the Lawlers Tonalite, Liberty Granodiorite and Porphyry Granite, and is oversampled relative to its small distribution.

(3) Granodiorite to granite suites: Sr-undepleted, Y-depleted in the more mafic end-members, but becoming Sr-depleted and less Y-depleted with increasing SiO_2 (Fig. 6C); SiO_2 65–74 wt% , with a distribution peak at 73 wt%. These suites are part of both 'external' and 'internal' granite groupings of Sofoulis (1988: *op. cit.*).

(4) Fractionated leucogranites to adamellites: Sr-depleted and Y-undepleted throughout their compositional range (Fig. 6D); SiO_2 69–78 wt%, with a maximum distribution at 75%. This group is part of the syn-kinematic and post-kinematic groupings of Bettenay (1988: *op. cit.*).

The more SiO_2-enriched end-members of groups 3 and 4 are difficult to distinguish.

The high Na contents and the Y-depleted trace-element patterns in the gneisses of group 1 and the more mafic granites of groups 2 and 3 are similar in part to those from granites associated with modern subduction zones, e.g. Papua New Guinea (Fig. 6E). However, the Yilgarn granites are far more enriched in SiO_2, K, Th and U. Trace-element patterns for group 4 are similar to Proterozoic anorogenic granites (Wyborn & others, in press: *Transactions of the Royal Society of Edinburgh*).

Implications for tectonic models

Tectonic models of the Yilgarn are based on analogues, either of subduction zones at a continental margin or extensional terranes. The rocks in the database, excluding the alkaline suites, have a bimodal SiO_2 distribution, characteristic of extensional terranes. Although chemically similar in some trace elements to granites of modern subduction zones, intrusives and volcanics of intermediate composition are not common, and the granite population is dominantly >70 wt% SiO_2. The data support the proposition of Groves & others (1987: *International Symposium on Granites and Associated Mineralizations, Brazil*) that the granites were derived by melting of an older felsic to intermediate crust, formed by lateral accretion during earlier events.

Implications for metallogeny

Traditionally, granites of the Yilgarn craton are not regarded as being metallogenically significant. However, the data from groups 2, 3 and 4 show rapidly increasing U, Y, Li and Rb with fractionation (Fig. 7): trends such as these occur in granites related to Sn and W mineralisation in Tasmania and north Queensland; and in the Cullen

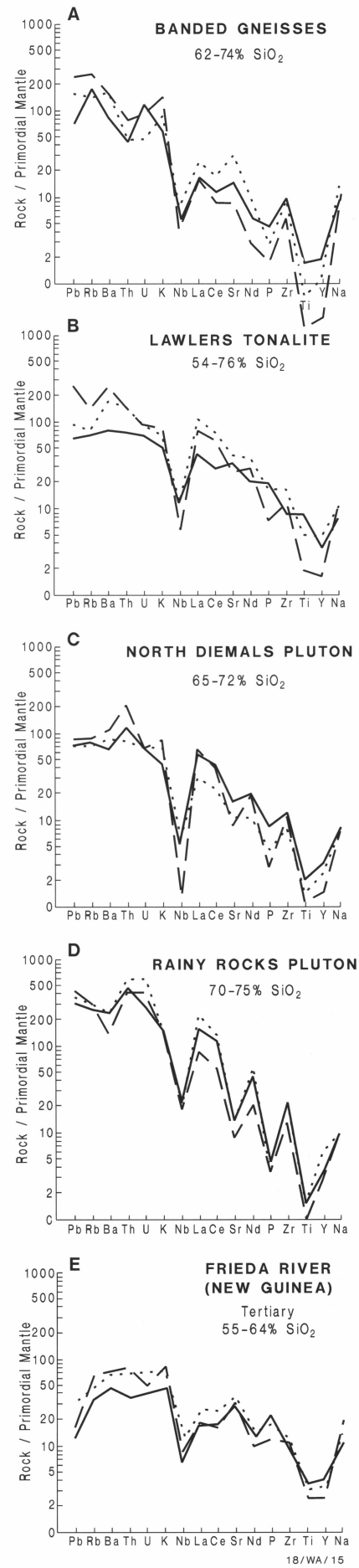

Fig. 6. Multi-element primordial mantle-normalised abundances for granites from the eastern Southern Cross and western Norseman–Wiluna Belt (A – group 1, B – group 2, C – group 3, D – group 4), and the Frieda River area (E – Papua New Guinea; data from Whalen & others, 1982: *Economic Geology*, 77, 592—616). Normalising values taken from Sun & McDonough, 1989: *Geological Society of London, Special Publication*, 42, 313–345. In any diagram, the straight line is the lowest SiO_2 content, the dotted line an intermediate SiO_2 content, and the dashed line the highest SiO_2 content.

Batholith of Northern Territory, where gold is present in the contact aureoles. This suggests that some Au mineralisation may be related to the granites, perhaps in a deposit style not yet defined in the Yilgarn Craton.

Implications for alteration

One unusual feature is the high Fe_2O_3/FeO ratios (>1) of some granite samples: Proterozoic granites with such ratios are invariably altered. These samples may correspond to linear lows commonly observed in airborne magnetic data over granite plutons. K and Na results are variable, being anomalously high in some samples and low in others. It is possible that regional mapping of these altered granites could define fluid pathways, which may be related to mineralisation.

Implications for lower crustal structure

The vast volume of granite exposed in the Yilgarn craton argues for a source of relatively uniform lower crustal felsic to intermediate composition. The present data suggest a dominance in the more mafic granite compositions of Sr-undepleted and Y-depleted granites, in contrast to those of Proterozoic age dominated by Sr-depleted and Y-undepleted types. Those provinces dominated by Sr-depleted granites have an intermediate-velocity layer at the crust/mantle boundary, whereas provinces dominated by Y-depleted granites have a sharp crust/mantle boundary (Wyborn & others, in press: *op. cit.*). The recent deep seismic traverse (reported elsewhere in this issue) shows a fairly uniform lower crust with a sharp crust/mantle boundary. The seismic data argue for a crust of felsic to intermediate composition, without the intermediate-velocity layer at the crust/mantle boundary, so characteristic of Proterozoic provinces.

Where to now?

Up to now, most geochemical studies of the Yilgarn have focussed on the greenstones; indeed, the database is dominated by mafic igneous rocks. This regional survey highlights the role of systematic regional geochemistry of both fresh and altered granites in any metallogenic or tectonic synthesis of the Yilgarn Craton, and shows that more granite data are needed.

More sampling sites should be selected, using regional geophysical data. Airborne magnetics clearly show major granite suites trending NNW, and the strong variation in K, Th and U content implies that airborne radiometrics should be able, in areas not chemically weathered or covered in alluvium, to discriminate the primary igneous suites and define alteration zones and the location of the more felsic fractionated plutons.

For further information, contact Dr Lesley Wyborn (Minerals and Land Use Program) at BMR.

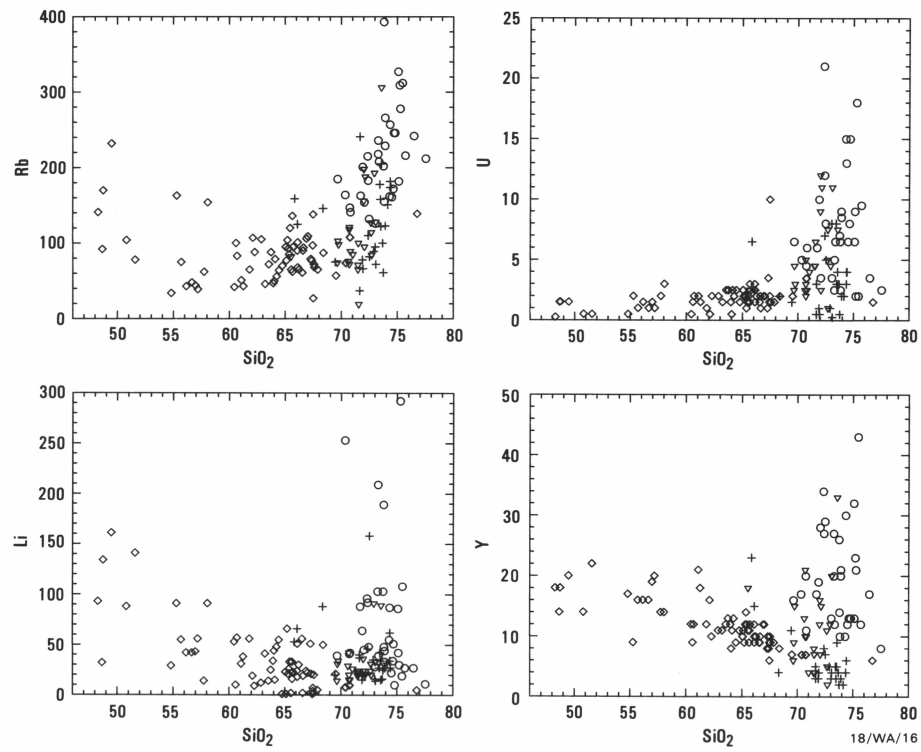

Fig 7. Harker variation diagrams. Crosses – group 1, diamonds – group 2, triangles – group 3, and circles – group 4.

Magmatic and metamorphic evolution and economic potential of the mafic/ultramafic Giles Complex, western Musgrave Block, W.A.

The late Proterozoic Giles Complex is one of the most extensive suites of layered mafic/ultramafic intrusions in the world. A detailed study, within the framework of the NGMA Musgrave Project, indicates that this complex consists of a number of discrete primary intrusive bodies rather than tectonic slices of a single Bushveld-type lopolith.

Magmatic evolution

The Giles Complex comprises several types of layered intrusions, including large gabbroic bodies (10–40 km along strike) with a small or no ultramafic component, e.g. Jameson, Blackstone, Cavanagh, Bell Rock, Hinckley, Michael Hills, and Mount Davies; and small to medium-sized layered intrusions (<10km along strike) with a significant ultramafic component, e.g. Murray Range, southern Mount West, Ewarara, Kalka, Gosse Pile, and Claude Hills (Fig. 8).

The Wingellina Hills body, one of the latter class of intrusions, consists of a poorly fractionated sequence of dunite, wehrlite, pyroxenite, gabbro, and gabbronorite. Chemical fractionation is limited: the Mg number (Mg/Mg+Fe) of olivine and orthopyroxene range from 0.89 at the base to 0.74 at the top of the intrusion. Orthopyroxene replaces olivine on the liquidus at Mg numbers of about 0.77–0.78.

Microprobe data have shown a multiple intrusive history for the Wingellina Hills body, with batches of olivine–spinel-saturated parent magma periodically emplaced into cooler and more evolved orthopyroxene–clinopyroxene–plagioclase-saturated resident magma. Intrusive events are recognised by coarse-grained ultramafic orthocumulate horizons resting on a partly resorbed fine-grained footwall of fractionated gabbronoritic adcumulates. These contacts are marked by sharp reversals in the composition of olivine, plagioclase, and clinopyroxene.

Microprobe data are available for about 300 samples from cross-sections through the major layered mafic/ultramafic intrusions of the Giles Complex in Western Australia. These intrusions include the Hinckley Range gabbro, Latitude Hill layered intrusion (a sliver of the Michael Hills gabbro), Bell Rock gabbro, southern Mount West, Blackstone gabbro, Murray Range layered intrusion, and Jameson gabbro (Fig. 8). A comprehensive report will be available soon. Some major results and their implications for magmatic evolution of the Giles Complex are:

(1) The layered mafic/ultramafic bodies experienced a multiple-intrusive history, as documented in Wingellina Hills, where fractionated gabbronorite resident magma was periodically replenished by batches of more

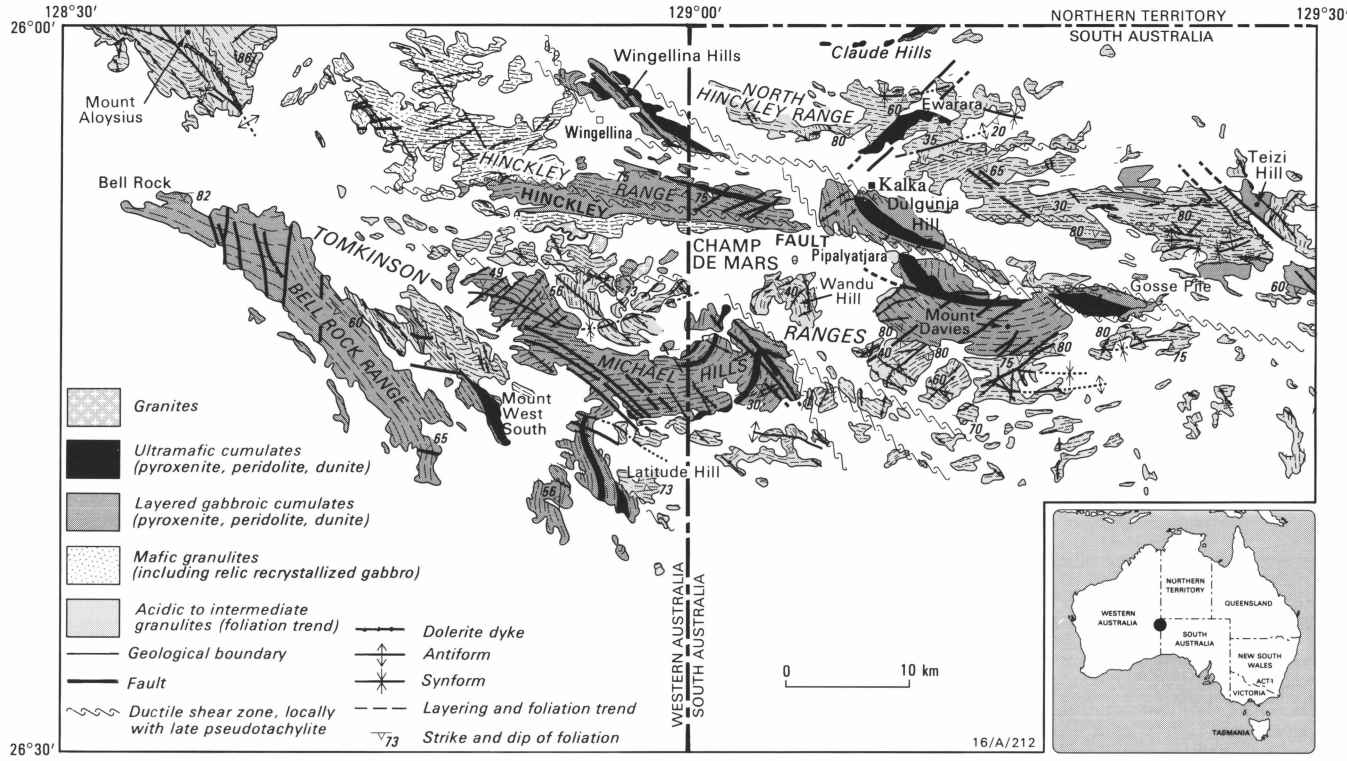

Fig. 8. The Giles Complex and environs, Tomkinson Ranges, western Musgrave Block, central Australia. The Blackstone Range, Cavanagh Range, Murray Range, and Jameson Range are west of the map.

primitive olivine-saturated melt. Similar relationships exist in other bodies with a significant ultramafic component, e.g. the Murray Range, southern Mount West, and Latitude Hill layered intrusions.

(2) The intrusions crystallised from several distinct magma compositions of different degrees of fractionation, all related to a single parent magma. The Mg number at which olivine is replaced by orthopyroxene on the liquidus is positively related to the silica activity of the melt, in turn reflecting the fractionation and assimilation history of the parent magma. The Wingellina Hills, Murray Range and southern Mount West intrusions were derived from an unfractionated hypersthene-normative Mid-Ocean Ridge Basalt-type magma, with orthopyroxene replacing olivine at an Mg number of about 0.78–0.76 (Fig. 9); a composition possibly close to the parent magma. The Bell Rock, Jameson, and Blackstone gabbros were derived from fractionated olivine (nepheline) normative melts, with the most primitive olivine having an Mg number around 0.67, persisting down to 0.55–0.50. The Latitude Hill and Hinckley intrusions fall between these extremes, with Mg values of 0.82–0.65.

(3) The intrusions display an exponential increase in fractionation of their cumulus phases within about 200 m of their present hanging-wall contacts, suggesting that the present upper contacts approximate the original upper intrusive boundaries and that each intrusion followed its liquid line of descent, intermittently interrupted by replenishment.

(4) The penetrative dyke swarm within the Giles Complex includes compositions that may be correlated with those of the parental precursor and derivative magmas of the layered intrusions. Phenocryst compositions and crystallisation sequences in these dykes match those in the spatially associated intrusions.

(5) The intrusions display at least two generations of gabbro: relic concordant units of microgabbro up to a few metres thick; and massive medium to coarse-grained gabbro. In volume, the microgabbro is minor to very minor in contrast to the medium-grained gabbro. It appears that the main intrusions were preceded by small and more rapidly cooled gabbroic pulses.

The above suggest that the present structural pattern of the layered intrusions closely reflects the shapes of the original magmatic bodies, related only through magma parentage, i.e. they are not slices of one Bushveld-

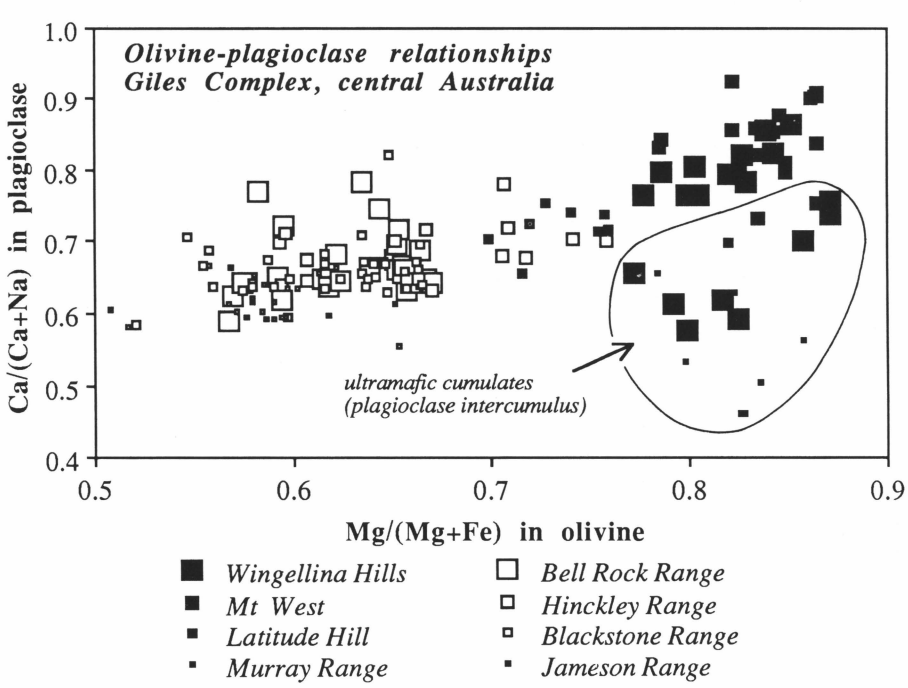

Fig. 9. Chemical covariation of olivine and plagioclase in the Giles Complex. Each data point represents the average of at least three microprobe analyses of olivine and plagioclase. The most fractionated olivine composition in each intrusion marks the point where the evolving melt reached the olivine–orthopyroxene cotectic, i.e. where olivine was replaced by orthopyroxene on the liquidus. Thus, the southern Mount West intrusion (0.79), Murray Range intrusion (0.78), Wingellina Hills layered intrusion (0.77), Latitude Hill intrusion (0.7), Hinckley Range gabbro (0.65), Bell Rock gabbro (0.56), Blackstone gabbro (0.52), and Jameson Range gabbro (0.5) were derived from magma batches progressively depleted in orthopyroxene, and have decreasing Mg number and silica activity.

like lopolith. The exponential increase in fractionation at the upper contact of most intrusions indicates that each intrusion represents a discrete magma chamber that followed its own fractionation path.

Phase equilibrium considerations demand that, once olivine is replaced on the liquidus by orthopyroxene (Fig. 9), the magma cannot revert to olivine-normative conditions, and simultaneously continue its normal fractionation path with respect to the Mg number of olivine and orthopyroxene and the Ca/Ca+Na ratio of plagioclase. The olivine/plagioclase relations are best explained in terms of high-pressure orthopyroxene (± clinopyroxene) fractionation of a common parent; i.e. the source magma of gabbroic intrusions (Blackstone, Bell Rock and Jameson) suffered extensive orthopyroxene fractionation at greater depth before emplacement. The Giles Complex is thus defined as a series of discrete coeval intrusions, sills and associated feeder dykes related through a common magma parentage.

Metamorphic history

The Giles Complex has long been cited as an example of high-pressure crystallisation and emplacement of basaltic magmas into lower to middle crustal levels, on the following basis: (1) Olivine, plagioclase, and magmatic spinel have reacted to form aluminous pyroxene and spinel; (2) clinopyroxene and orthopyroxene are enriched in Ca–Al and Mg–Al Tschermak components; and (3) in some ultramafic cumulates, plagioclase is one of the most potassic calcic antiperthites ($An_{75}Ab_5Or_{20}$) reported from terrestrial cumulates. These observations are consistent with high crystallisation pressure, extremely high crystallisation temperatures (owing to high confining pressure), and rapid near-isobaric cooling.

A thermobarometric study of cumulates from the Wingellina Hills intrusion exhibiting varying degrees of fractionation has essentially confirmed the original concept of high-pressure crystallisation of Goode & Moore (1975: *Contributions to Mineralogy and Petrology,* 51, 77–97), but has significantly reduced the previous pressure estimates (10–12 kbar) to around 6 kbar (Ballhaus & Berry, 1991: *Journal of Petrology*, 32, 1–28), equivalent to an emplacement depth of about 20 km.

These high-pressure features have previously been recorded only from layered intrusions north of the Hinckley fault, including the Wingellina Hills, Kalka, Ewarara, Gosse Pile, Teizi, and, possibly, Claude Hills intrusions. In other intrusions, olivine and plagioclase are in stable coexistence, except for rare amphibole–spinel coronas at olivine–plagioclase contacts in altered units in the southern Mount West body. Consequently, it has been postulated that intrusions south of the Hinckley fault have been emplaced at shallower crustal levels (Nesbitt & others, 1970: *Geological Society of South Africa, Special Publication*, 1: 547–564; Goode & Moore, 1975: *Contributions to Mineralogy and Petrology*, 51: 77–97). However, the present study indicates that the 'low-pressure' intrusions, i.e. those lacking spinel coronas around olivine, are cut by primitive olivine–plagioclase dykes that include phenocrysts showing reaction relations with one another and with devitrified groundmass. The lack of high-pressure reaction textures in some intrusions may be a consequence of phase compositions unfavourable for the development of spinel coronas and, thus, does not necessarily indicate emplacement at shallower crustal levels.

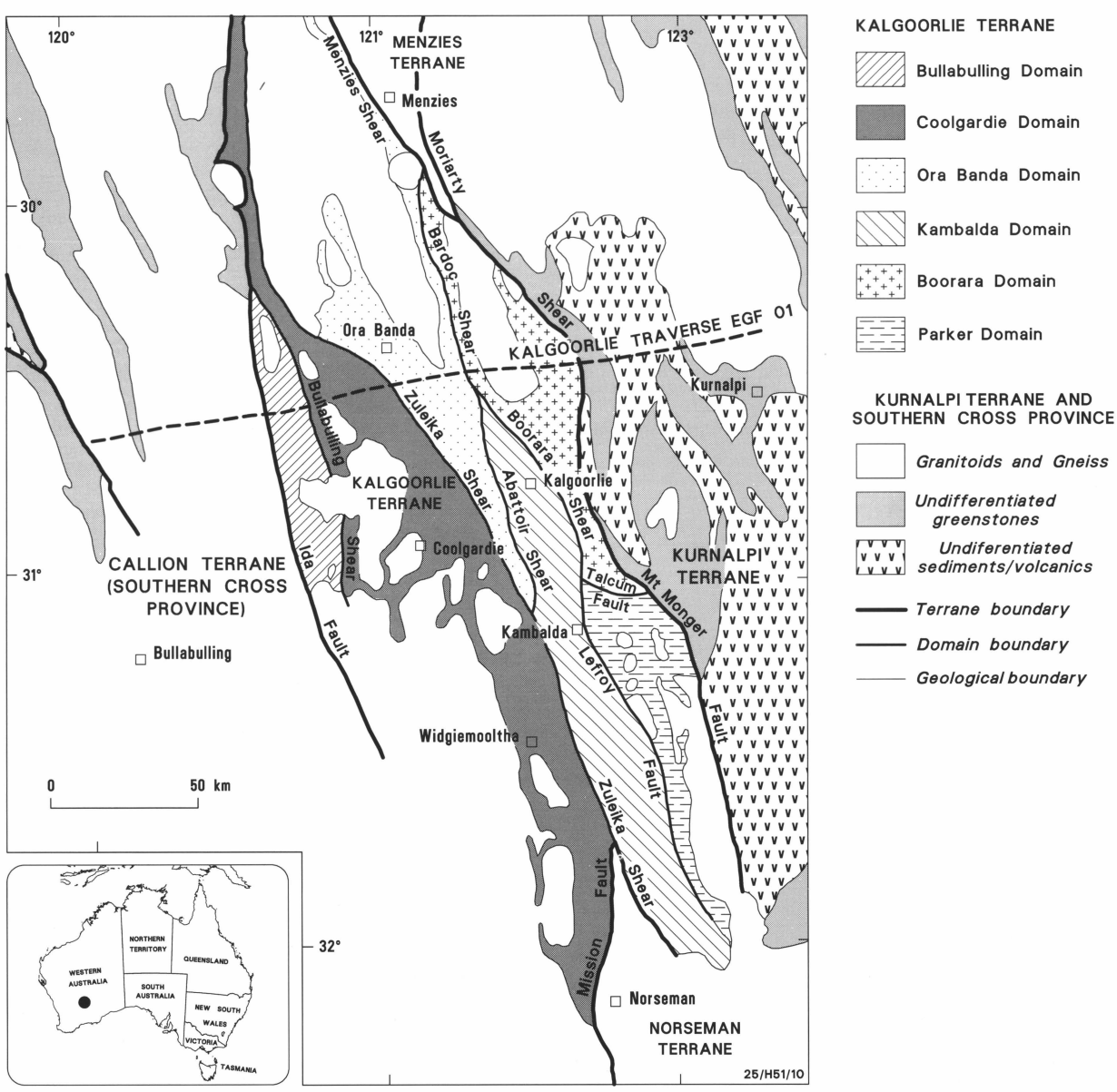

Implications for mineralisation

Selected samples from the well-studied cumulate suite of the Wingellina Hills intrusion have been analysed, in collaboration with R.R. Keays, University of Melbourne, for the Platinum Group Elements (PGE: Pt, Pd, Ir, Ru) and Au. The highest value of 30 ppb combined PGE (Pd>Pt) occur in the most primitive ultramafic units, just above horizons of magma replenishment, dropping rapidly to below 3 ppb in more fractionated gabbroic cumulates. The widely disseminated sulphides in ultramafic cumulates suggest that the most primitive derivatives of the parental magmas of the Giles Complex were sulphur-saturated upon emplacement. Since early saturation in sulphide does not generally allow effective concentration of PGE, the geochemical data documented so far from the Giles Complex leave open the question of the economic significance of these layered intrusions.

For further information contact Dr C.G. Ballhaus (Institute of E Mineralogy and Petrography, Albert-Ludwigs Universitat, G Freiburg, D7800, F.R. Germany), or Dr A.Y. Glikson, Minerals and Land Use Program, BMR.

1991 Eastern Goldfields seismic reflection survey

Deep seismic reflection data from the Archaean Eastern Goldfields region of Western Australia clearly show that the greenstone belts are a thin, flat-bottomed sequence, superimposed on an otherwise uniformly thick crust.

A seismic reflection survey to map the three-dimensional geometry of the Eastern Goldfields greenstone belts was carried out in mid-1991 by BMR and the Geological Survey of Western Australia, as part of the National Geoscience Mapping Accord (Fig. 10).

In particular, the survey was concerned with the shape and thickness of the greenstones, the geometry of boundary faults, internal shear zones, and intrusive granites within the greenstone belts, and the greenstone's structural relations with adjacent granitic rocks. A study was made of structure, form and crustal thickness between the Eastern Goldfields and Southern Cross Provinces, as a means of comparing and understanding tectonic evolution.

The seismic traverse, 30 km north of Kalgoorlie, was 213 km long, and oriented east–west to cross the Eastern Goldfields greenstone sequences and extend into the granitic rocks of the Southern Cross Province. These sequences have been subdivided into two main terranes, the Kalgoorlie and Kurnalpi terranes (Fig. 10), which in turn have been subdivided into domains bounded by mineralised shear zones.

Seismic results

From the seismic data we have deduced that the greenstones are, in general, 6 km thick, although in places they reach 9 km. They have a predominantly planar base, and variations in greenstone thickness appear to have resulted from block faulting (Fig. 11).

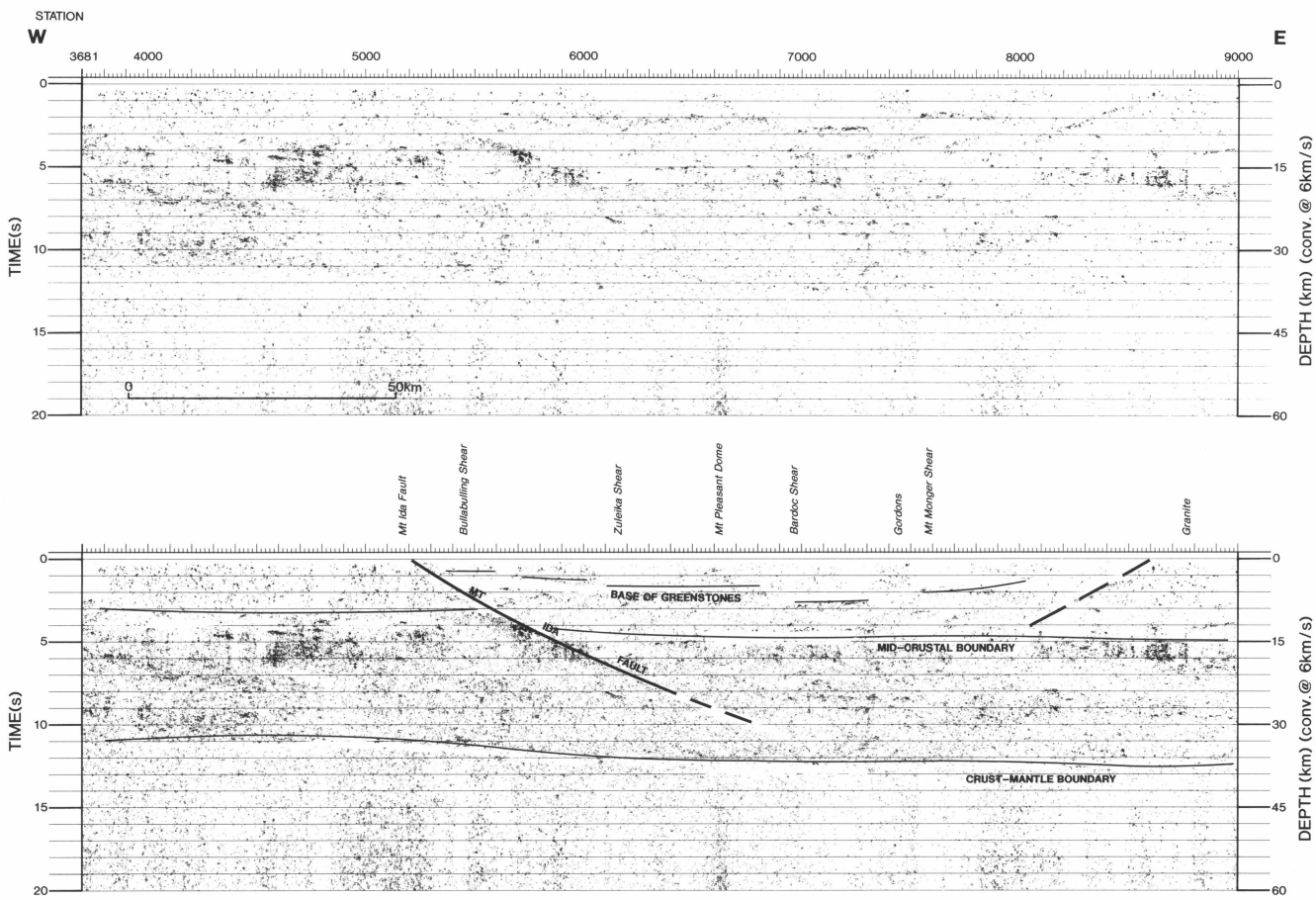

Fig. 11. Interpreted seismic reflection section from the Eastern Goldfields region of Western Australia. The main features observed on the seismic section are the flat-base to the greenstones, the planar nature of the Mount Ida Fault, the uniformity of the mid-crust beneath the greenstone and granite regions, and the shape of the crust/mantle boundary.

(Opposite page)

Fig. 10. Geological map of the Eastern Goldfields region, with major structural sub-divisions. Modified from Swager & others (1990), '*Geology of the Archaean Kalgoorlie Terrane*', 1:250 000. Geological Survey of Western Australia. The position of the 1991 Eastern Goldfields seismic traverse is shown.

The Mount Ida Fault forms the greenstone's western boundary. It is clearly imaged in the seismic data (Fig. 11) as a moderately dipping planar reflector, plunging east at approximately 25–30° to deeper than 25 km. The eastern boundary of the Kalgoorlie Terrane has been mapped at the Mount Monger Fault, which, however, does not show on the seismic data. A strong planar reflector dipping west at around 30 has been imaged (Fig. 11). This reflector correlates with the contact between the granite at Arcoona and the Kurnalpi Terrane.

The seismic data have imaged some of the internal structure of the domain boundary shear zones in the Kalgoorlie and Kurnalpi Terranes. These zones have a significant re-

gional extent, but their depth extent was previously unknown. The block faulting seen at the base of the greenstones relates to the location of known major mineralised shear zones. Further detailed processing is aimed at resolving the structural relationship between the block faulting and the internal boundary shear zones.

The upper surface of the sub-cropping Goongarrie Granite Dome, the Mount Pleasant Dome (Fig. 11), is imaged as a domal reflector beneath a sequence of mafic and ultramafic rocks, which are domed above the granite. The base of this granite is less-well resolved in the seismic data, but is believed to be a set of sub-horizontal reflectors just less than 6 km deep. The seismic data indicate that most granites within the greenstone belts, including post-tectonic types, have a lenticular shape.

The difference in reflection character of the upper and middle crust beneath Southern Cross region and the Eastern Goldfields region is minimal, suggesting a uniform crust beneath both regions. This implies that the greenstones were deposited on a predominantly felsic crust, which has bowed isostatically to compensate for the addition of higher density greenstone.

The data suggest the greenstones formed by ponding in a basin that resulted from extension on the Mount Ida Fault, a major crustal shear. An implication of this simple model is that more shear zones must occur east of the Mount Ida Fault to account for the current width of the greenstone basin.

For further information, contact Dr Bruce Goleby, Dr Barry Drummond (Onshore Sedimentary & Petroleum Geology Program), Dr Peter Williams (Minerals & Land Use Program) at BMR, or Dr Cees Swager (Geological Survey of Western Australia).

Geological investigations in the Kimberley–Arunta region

During the second year of the National Geoscience Mapping Accord Kimberley–Arunta project, BMR and the Northern Territory Geological Survey have concentrated on mapping and synthesising data from MOUNT DOREEN* and HERMANNSBURG (Fig. 12), thus providing new insights into the evolution of the Arunta Block.

* Names of 1:250 000 Sheet areas are printed in capital letters.

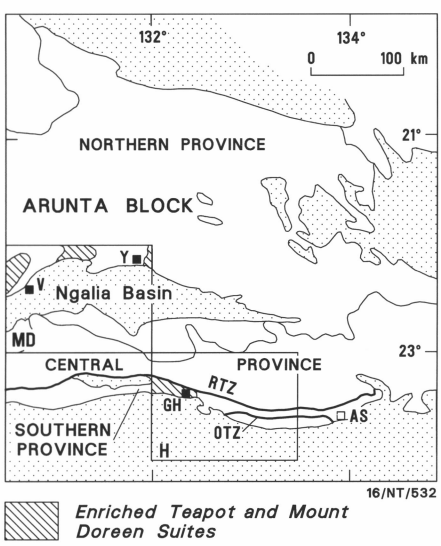

Fig. 12. The three provinces of the Arunta Block and the distribution of felsic suites in HERMANNSBURG (H) and MOUNT DOREEN (MD). AS – Alice Springs; GH – Glen Helen homestead; OTZ – Ormiston Thrust Zone; RTZ – Redbank Thrust Zone; V – Vaughan Spring homestead; Y – Yuendumu township.

The preliminary solid geology map of MOUNT DOREEN (Fig. 13) is based on exposed features plus airborne magnetic, three-channel radiometric (1.6 km line spacing) and Bouguer gravity data.

Of particular interest is a series of migmatitic gneiss bodies, which appear to be basement, but may represent a discordant, younger envelope of high-strain and high-grade metamorphism. They are traceable discontinuously westward from northeast of Yuendumu, and commonly crop out near gneissic granite plutons rich in mafic and country rock xenoliths (Fig. 13). The gneissic rocks are concentrated in a region where greenschist facies metamorphism extended above the biotite isograd and where the Lander Rock beds, a widely distributed unit of immature sandstone and siltstone (Fig. 13), show upright folds with an axial planar crenulation cleavage. An earlier phase of tight to isoclinal folds in the same unit, with slaty cleavage as the axial plane structure, may be the result of thrusting and crustal shortening. Studies are continuing on various tectonic models to explain these features and, in particular, determine the age and heat source for migmatisation.

Two other granite suites with economic potential have been identified, both comprising late-stage granites with considerable enrichment in U, Th, Rb and REE compared to normal Proterozoic granites of northern Australia, such as the Kalkadoon Granite. Their geochemistry is consistent with formation during second-stage melting in the lower crust at unusually high temperatures, and both are typically Sr-depleted and Y-enriched, like most Proterozoic granites in northern Australia.

One suite, represented by the Teapot Granitoid Complex in HERMANNSBURG, is commonly surrounded by a wide (up to 5 km) migmatisation zone, suggesting that the granite originated by mid-crustal melting. A mixed

Fig. 13. Preliminary solid geology map of the Mount Doreen 1:250 000 Sheet area.

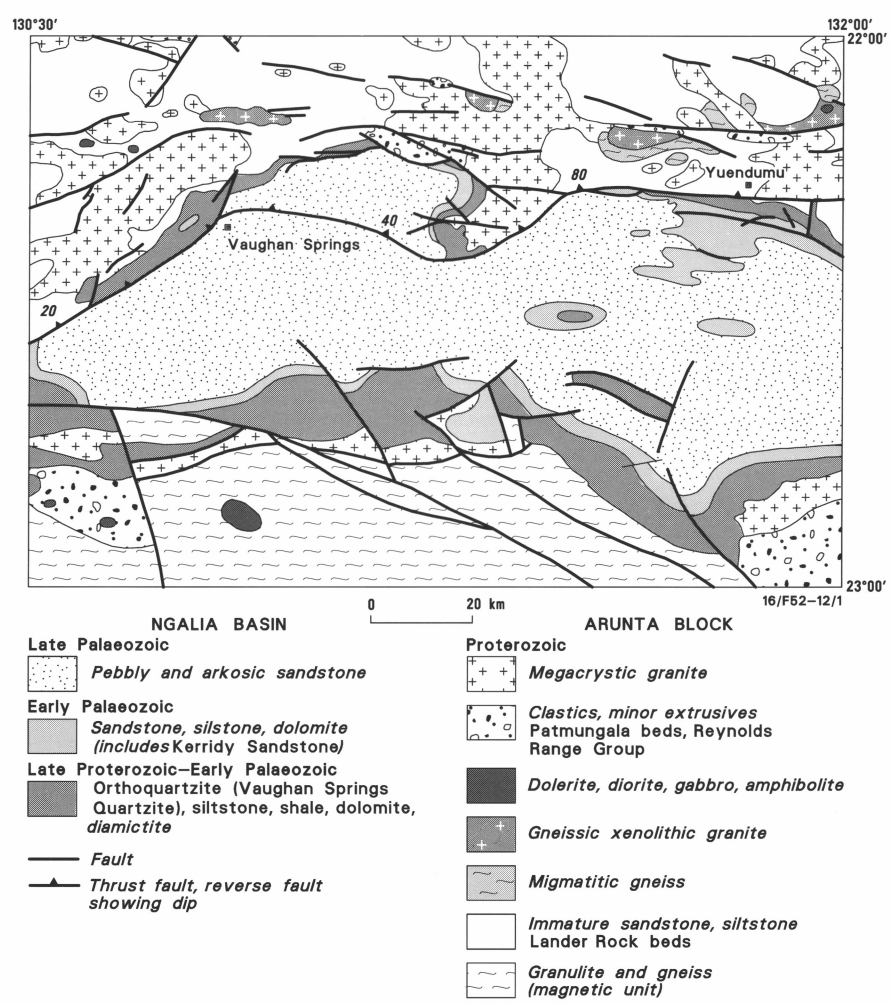

source region is indicated by Sm–Nd isotopic studies now in progress. Relatively low values in F, Li, Sr and Sn may reflect local I-type source characteristics.

The other enriched suite, exemplified by the Mount Doreen Granite, is characterised by both megacrystic K-feldspar and biotite. It is widespread in MOUNT DOREEN, where it forms high-level, cross-cutting, post-metamorphic plutons, and has some small wolframite and copper deposits spatially related to it. The uranium in the Palaeozoic sedimentary succession of the Ngalia Basin was probably derived from these granites by erosion, transportation in groundwater, dissolution and precipitation.

Mineralogical features, such as the presence of tabular feldspars, biotite and fluorite, and their radiometric signature, indicating above average U, Th and K, suggest that this granite suite was generated by second-stage melting from an S-type source (Warren & Sun 1992: *Abstract, 2nd Hutton Symposium, Canberra*). From the above features and preliminary geochemical data, this northern granite suite is predicted to have higher F, Sn and Li, and very much lower Sr contents, compared to the southern suite, and to be closely related to granites in NAPPERBY, MOUNT PEAKE and BARROW CREEK, to the northeast.

The current work has reinforced previous ideas on stratigraphic correlation between the Arunta Block, Tennant Creek Inlier, and The Granites–Tanami region (Table 2). The importance of this is that rocks of similar age, composition, and metamorphic grade to those associated with gold mineralisation at Tennant Creek and in The Granites–Tanami region probably occupy large parts of the northern Arunta Block, thus vastly expanding the potential area for gold.

Structural and stratigraphic mapping support reflection seismic evidence that the mid to Late Palaeozoic tectonism in and around the Ngalia Basin is characterised by widely spaced, low-angle thrust faults and high-angle reverse faults. The faults cut basement and are not linked by flat detachment zones.

These features are consistent with the view that thick-skinned tectonics dominated. However, a minor amount of thin-skinned detachment is recognised in the lower part of the Vaughan Springs Quartzite, near the base of the Ngalia Basin succession, possibly facilitated by evaporitic units in the succession (suggested by salt efflorescences on siltstone exposures).

An unsolved problem in MOUNT DOREEN is the stratigraphic position of a unit of felsic and mafic granulite and gneiss south of the Ngalia Basin (Table 2; Fig. 13). Although the unit is known from only one exposure, its magnetic signature indicates that it is part of a broad belt characterising the central province of the Arunta Block (Fig. 12), and thought to represent mainly metamorphosed and deformed extrusives. These metamporphics, which reached peak PT conditions of 81 Kb and 700–800°C, were folded and intruded by granite at about 1750 Ma (Black & Shaw, 1991: *Australian Journal of Earth Sciences*, 38, 307–332). The age of the protoliths is unknown. The granulite and gneiss appear to be overlain by schist, which may represent a distal equivalent of the Reynolds Range Group, as suggested by Stewart & others (1984: *Australian Journal of Earth Sciences*, 31, 445—455), although lithologically it resembles schist of the Lander Rock beds.

Age (Ma)	The Granites–Tanami region	Northern Arunta Block	Tennant Creek Inlier
~ 1560		Megacrystic granites, Teapot Granitoid Complex	
~ 1600	Birrindudu Group		Tomkinson Creek beds
~ 1750	**STRANGWAYS**	**TECTONIC**	**EVENT**
~ 1800	Mt Winnecke Formation	Patmungala beds, Reynolds Range Group	Hatches Creek Group
		Gneissic granites	
~ 1850	**UNNAMED**	**TECTONIC**	**EVENT**
~ 1870	Tanami Complex	Lander Rock beds	Warramunga Group
?		Granulite and gneiss	

Table 2. Stratigraphic correlations.

For further information, contact Drs Russell Shaw, David Blake, Gladys Warren, or Shen-Su Sun (Minerals & Land Use Program) at BMR; or Mr David Young at NTGS, Alice Springs.

Giant sediment-hosted Pb–Zn deposits: what drives metal enrichment?

Proterozoic Pb–Zn deposits, such as Broken Hill, Mount Isa, Hilton, the yet unexploited HYC deposit at McArthur River, and the recent discovery at Century, are an important part of Australia's mineral wealth. The very magnitude of these deposits, typically more than 10 Mt of combined Pb and Zn, presents a serious geochemical problem in an apparently straightforward model of sedimentary to early diagenetic ('sedex') ore formation.

Compaction-driven 'basin dewatering' is widely seen as a simple mechanism to form sediment-hosted base-metal ores, including the giant stratiform Pb–Zn deposits. However, the available geological information from the best-preserved Australian example, the HYC deposit in the McArthur Basin (Logan & others, 1990, *AusIMM Monograph* 14, 907–911), and geochemical modelling of Pb and Zn solubility discussed below, suggests that the quantity of fluid trapped within the basin sediments may have been insufficient to transport enough Pb, Zn, and reduced S in a single solution at normal basin temperatures — even if the entire fluid volume was discharged rapidly through a perfect focus along a fault (Solomon & Heinrich, 1992: *Exploration and Mining Geology*, 1, 85–91). Published research on the evolution of modern intracontinental basins in North America further indicates that sediment dewatering is typically slow and defocussed, and thus inherently unfavourable for the formation of large ore deposits (Bethke, 1986: *Economic Geology*, 81, 233–249).

Several lines of evidence suggest that an extra source of *energy* may be essential for the formation of a giant sediment-hosted Pb–Zn deposit: either a source of heat to enhance metal solubility, or a mechanical driving force to boost fluid flow, or both. Given an effective plumbing system through faults, the type and location of this energy could exert a major control on where a giant deposit may form.

Base-metal and S solubility in the source region and along the transport path of the hydrothermal fluids is arguably the single most important variable in any model for the chemical enrichment. Metal solubilities can vary by at least six orders of magnitude for geologically quite realistic assumptions of fluid salinity, source rock mineralogy, and fluid source temperature.

Salinity raises the solubility of Pb and Zn sulphide by at least a factor of 10 for each doubling of total salt concentration, because chloride acts as transporting ligand for Pb and Zn, and the acidity of a rock-buffered fluid increases in proportion with fluid salinity (below). An obvious potential source of salt is the abundant evaporitic sediments in the McArthur Basin and other basins that contain stratiform base-metal deposits. Evaporites are probably one essential ingredient for the formation of giant Pb–Zn deposits, both appearing together in the geological record about 1800 Ma ago.

The *mineralogy of the fluid source rocks*

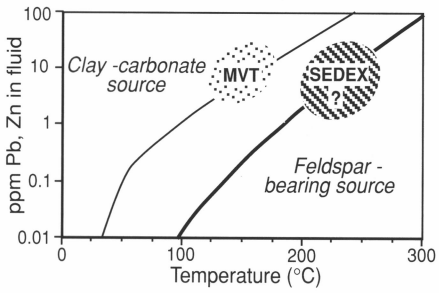

Fig. 14. Pb and Zn solubility in a basin brine with 25% total salinity, assuming optimal conditions for co-transportation of metals and reduced S (equal molalities of $m_{Pb} = m_{Zn} = m_{H2S}$). Note that base-metal solubility strongly depends on temperature and on the Al silicate mineralogy of the source rocks.

affects metal solubility, firstly because equilibria between a fluid of given total salinity and Al silicates in the rock act as acidity buffers. Widespread clastic feldspar in rocks of the McArthur basin buffers the acidity of brines to near-neutral pH, and thereby constrains maximum Pb, Zn, and sulphide solubility to relatively low values (Fig. 14). This could be one of several metallogenically significant differences to the Canning Basin, which hosts Mississippi Valley Type Zn (–Pb) deposits with a comparable aggregate metal content, but which may have major clay and carbonate-rich formations at depth (see *BMR Research Newsletter* 12; and Jaireth & others, *BMR Record* 1990/38). The absence of feldspars in potential fluid source rocks within the Canning Basin could allow basin fluids to be more acid, and thus enhance Pb and Zn solubility by an order of magnitude (at a given salinity and temperature) compared with the feldspar-buffered fluids expected in the McArthur Basin (Fig. 14). Secondly, the mineralogy in the source and along the flow path of the brines affects their S content and redox potential: low concentration of reduced S could allow higher Pb and Zn concentrations, which would solve the chemical transport problem without any specialised energy source. However, S isotope data from the HYC deposit are most easily interpreted as indicating co-transportation of Pb + Zn + reduced S in a single ore fluid.

If these interpretations are correct, then an elevated *temperature* in the fluid source region (coupled with a mechanism of rapid fluid transport to the deposition site, in order to limit cooling) becomes a key limiting factor for ore formation, because base-metal solubility increases exponentially with temperature (by a factor of 10 for a rise of about 35°C; Fig. 14). A minimum of 200–250°C is required to transport realistic concentrations of 10 ppm Pb and Zn, plus an equivalent concentration of sulphide, in a basin brine in equilibrium with feldspar. Tentative fluid inclusion evidence from McArthur River indeed suggests relatively high fluid temperatures.

Given that the sedimentary sequence beneath the HYC deposit is at most 5 km thick, we conclude that the ore-forming fluids have interacted with the basement beneath the McArthur Group to attain such high temperatures; this is consistent with (but not proven by) published Pb isotope data from the McArthur Basin (Gulson, 1985: *Economic Geology*, 80, 2001–2012). Similar, but more conclusive, evidence for high fluid temperatures and basement-derived Pb has been obtained from the giant Pb–Zn deposits in Ireland, which also have other similarities with the Australian examples.

The energy source driving such deep fluid penetration is unknown. Primarily mechanical energy may be supplied by large-scale tectonics, which, through topographic uplift or by suction effects in active faults, may drive evaporitic brines deep into the crystalline basement and back to the surface. Alternatively, an additional heat source may be invoked. Granite magmatism would be effective, but there is no evidence for coeval magmatism. Radiogenic heat from older U-rich granites in the basement is produced more slowly, but may heat infiltrating fluids sufficiently to drive episodic fluid convection during times of tectonic fracturing of the basin and basement rocks. High heat-producing granites could provide a particularly attractive solution to the chemical mass transport problem discussed above, because they may not only provide a mechanical buoyancy force for episodic fluid flow, but will at the same time enhance base-metal solubilities by heating the ore fluids at the bottom of the convection cells. In the Mount Isa Inlier, later deformation and erosion of sediments of similar age and character as the McArthur Group have exposed high heat-producing granites underlying the Pb–Zn mineralised Mount Isa Group; for example the Sybella Granite near Mount Isa. The inference of similar 'hot' granites beneath HYC and other less-well exposed deposits remains speculative, but might be testable by measurements of fossil thermal gradients (e.g. carbon maturation or illite crystallinity studies).

More immediate questions about the ore fluids wait to be investigated, particularly the crucial mode of transport and oxidation state of S, and the temporal relation between fluid flow and fault movements. To better understand the physics and chemistry controlling the location of sediment-hosted base-metal deposits, MIM Exploration Pty Ltd is funding a research project at BMR. This will initially focus on the HYC deposit, as it is the least overprinted by deformation, metamorphism and later metasomatism. The one to two-year project will start in May 1992, and be carried out by Mark Hinman, who is currently completing his Ph.D. (James Cook University) on base and precious metal mineralisation in the Cobar area. The results of the HYC study, to be published after a confidentiality moratorium, will contribute to exploration and assessment of the base-metal potential of other Proterozoic regions.

For further information contact Dr Chris Heinrich or Dr Mike Solomon at BMR, or Mr Peter Stoker at MIM Exploration Pty Ltd in Brisbane.

Metal segregation by magmatic gases—first results from new fluid inclusion technique

BMR's Minerals and Land Use Program and CSIRO's Division of Exploration Geoscience are collaborating in the development and application of a new technique for quantitative analysis of metals in fluid inclusions. The proton microprobe, at CSIRO, now allows analysis of a single inclusion for base-metals and other heavy elements, down to trace levels near 50 ppm. This technological advance has already led to surprising results on metal transport in magmatic–hydrothermal ore systems, and is expected to make a major impact on metallogenic research. Once some baseline information on fluid compositions is available, the technique may become a highly specific exploration tool.

One of the first fluid inclusion applications of quantitative Proton Induced X-ray Emission (PIXE) spectrometry used a high-temperature quartz–cassiterite vein from the Mole Granite in New England. The vein has relatively large regular-shaped brine and vapour inclusions, previously described by detailed textural, isotopic and microthermometric measurements. These two inclusion types are probably near-pristine magmatic fluids that coexisted with the source granite at 500–600°C before being trapped at somewhat lower temperature (Sun & Eadington, 1987, *Economic Geology*, 82, 43–52).

The high-salinity inclusions, showing a small bubble and a halite crystal at room temperature (Fig. 15), contain Na, Cl, K, Fe, Zn and Mn at weight percent levels, plus 300–3000 ppm Cu, Pb, Sn, As and other heavy metals. Metal-concentration ratios in the brine, when compared with the corresponding average element-concentration ratios in the Mole Granite, agree with published experimental distribution constants between chloride fluids and silicate melts. This indicates that the fluids were probably exsolved directly from the crystallising Mole Granite magma, thus confirming chemical models for granite-related Sn–W–base-metal mineralisation derived from thermodynamic calculations (Heinrich, 1990: *Economic Geology*, 85, 457–481).

Large-bubbled primary vapour inclusions in the same sample contain a small opaque daughter crystal (probably a copper sulphide; Fig. 15), and have a total salinity and density consistent with derivation by fluid phase separation from the same

magmatic–hydrothermal system. Compared with the coexisting brine inclusions, they have elevated CO_2, as determined by Raman microspectrometry, and a high total sulphur content, as indicated by semiquantitative proton microprobe analysis. They show low concentrations of most heavy elements but, quite unexpectedly, a very high Cu content—about 1 wt% Cu. Ratios like Cu/Fe, Cu/Zn and Cu/Pb in the vapour are 2–3 orders of magnitude higher than in the brine inclusions. Published thermodynamic estimates and reconnaissance experiments have indicated significant Cu volatility as gaseous Cu–Cl complexes, but the magnitude of base-metal partitioning between brine and vapour, shown by the analytical data from the Mole Granite, requires a more fundamental difference in complexation behaviour of Cu between the two fluids. The data are plausibly explained by relatively volatile Cu"S complexes, causing preferential partitioning of Cu and S into the vapour phase, while chloride-complexed metals (like Fe, Zn, and other transition metals) remain in the chloride-rich brine. Base-metal segregation resulting from progressive high-temperature fluid phase separation might thus be a crucial enrichment step in the formation of magmatic–hydrothermal ore deposits. This possibility has so far not generally been considered and may be of particular importance to porphyry-Cu mineralisation. Further analytical, as well as experimental, work is required to test this possibility.

Au, even more so than Cu, can be expected to partition into the vapour phase in a S-rich high-temperature brine + vapour system. This may provide an effective Au (–Cu) enrichment step in the mineralisation of granite-related breccia pipes, and possibly of some epithermal kaolinite–alunite-type Au (–Cu–As) systems. A recent textural, fluid-inclusion and stable-isotope study of the breccia-hosted Au deposit at Kidston in north Queensland (Baker & Andrew, *Economic Geology*, 86, 810–830) independently suggested that a magmatic gas condensate acted as the main Au-precipitating fluid (rather than the magmatic brine or late meteoric fluids that were both present in the breccia system at some stage).

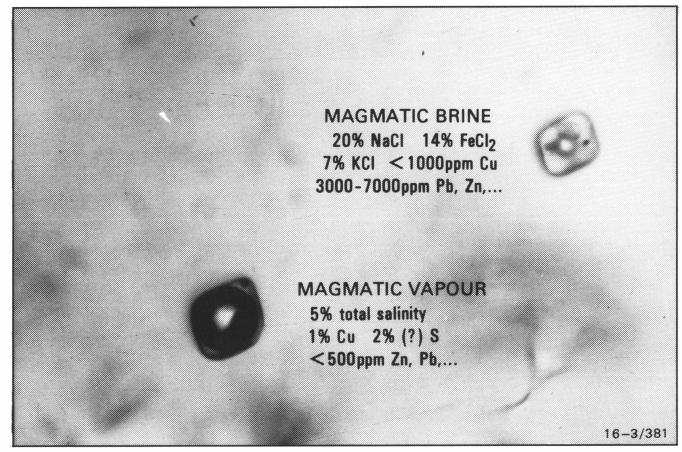

Fig. 15. Photomicrograph of coexisting high-temperature magmatic brine and vapour inclusions in quartz from Yankee Lode, a cassiterite deposit in the Mole Granite, New England. PIXE analyses of individual inclusions demonstrate strong fractionation of Cu in favour of the S-bearing vapour phase, while most other heavy metals are enriched in the chloride brine.

Ongoing proton microprobe studies will focus on reconnaissance analysis of fluid inclusions from porphyry-Cu deposits, and on applications to Archaean Au mineralisation to contribute metallogenic data to the Eastern Goldfields NGMA project. We would welcome any proposals from the mineral industry to collaborate in continual development and application of the technique, and to broaden our baseline data.

For further information, contact Dr Chris Heinrich or Dr Terry Mernagh at BMR (Minerals and Land Use Program), or Dr Chris Ryan at CSIRO (HIAF Centre) in North Ryde.

The Williams and Naraku Batholiths, Mt Isa Inlier: an analogue of the Olympic Dam Granites?

The last major felsic plutonic event in the Mount Isa Inlier was the emplacement of high-uranium I-type granites to form the Williams and Naraku Batholiths. These 1560–1480 Ma granites are mineralogically and chemically distinct from any other felsic intrusives in the Mount Isa Inlier, and show the best evidence for crystal fractionation producing a series of coeval, but compositionally distinct, plutons, which range from zoned plutons with coarse magnetite–hornblende-bearing rims and felsic cores to high-SiO_2 plutons strongly enriched in U and Th. Widespread metasomatic alteration and brecciation of the country rocks and granite is associated with the more SiO_2-enriched phases. The alteration products are complex with end-members varying from pure albitite to rocks rich in K-feldspar and hematite. The Williams and Naraku Batholiths crop out over more than 2400 km^2 (Fig. 16) and are inferred from geophysical data to extend north and south of the Mount Isa Inlier beneath the Carpentaria, Eromanga and Georgina Basins. Deposits of Cu, Au, Ag and U occur both within and around their margins. In chemical composition and association with regional hematite-rich breccias, the batholiths closely resemble the granites of the Stuart Shelf Region, including the host rocks at Olympic Dam.

The batholiths contain at least two ages of granite intrusions. The older intrusions consist of small microgranite or trondhjemite bodies, predating the major deformation event (D2), which produced major N–S trending structures. The younger intrusions dominate the batholiths and were emplaced after D2, but are strongly foliated near major D3 structures, which form SSE or NNE-trending shear zones. This article is concerned only with the younger intrusions.

Compositional variation

The batholiths are extremely heterogeneous, and three genetic variables determined the mineralogical and chemical variations dealt with below.

(1) Primary magmatic variation. The Williams Batholith consists of a series of compositionally distinct granitic intrusions, which crystallised by convective fractionation (Sparks & others, 1984, *Philosophical Transactions of the Royal Society of London*, A310, 511–34). The more mafic minerals crystallised along the magma chamber walls and the derivative interstitial magmatic liquid, being less dense than the primary magma, ascended to the top of the chamber. Here, owing to the large density difference, the primary and derivative liquids were unable to mix and thus remained segregated. Periodically, the lighter, more SiO_2-enriched derivative liquid, may have moved upwards either to form a shallow intrusion and/or to be extruded as volcanics. The result of this style of crystallisation is a composite suite of zoned plutons, mafic plutons, and predominantly high-SiO_2 fractionated plutons. The more mafic granites are dominated by biotite ± hornblende ± magnetite, and most are reddish-pink, owing to hematite-dusted K-feldspar.

The Williams Batholith shows a strong north–south compositional variation, with the zoned and more mafic plutons predominating in the southern Selwyn/Mount Merlin 1:100 000 Sheet areas, and the high-SiO_2 granites in the Mount Angelay and Malbon Sheet areas (Fig. 16). The Naraku Batholith in the Cloncurry, Marraba and Quamby Sheet areas seems to be continuous with the Williams Batholith beneath the Proterozoic sediments of Cloncurry Sheet. Compared to other granites of the Mount Isa Inlier, both the Williams and Naraku granites contain high U, up to 30 ppm being common (Fig. 17). Na_2O and

incompatible elements, such as Nb (Fig. 17) and Zr, are also high.

In the higher SiO_2 parts of the Williams Batholith, K-rich aplite dykes are present: where they intrude the more mafic phases, they are either associated with massive hematite dykes at the contact, or zones of granite breccia with hematite and/or quartz dominant in the matrix. Where the high-SiO_2 plutons intrude calc-silicates, albitite dykes and pipes are common in the granite, extending into the country rock.

Regionally developed breccias, extending over 80 km along strike, are also present in both the high-SiO_2 granite and the country rock. Some of these breccias may be related to faulting, e.g. some are present along the Cloncurry Fault Zone on the Selwyn Sheet. However, most breccias on the Mount Angelay and Cloncurry Sheets (Fig. 16) appear to be located in the roof zone of the batholiths (Fig. 18).

(2) Chemical interaction with the adjacent country rocks. Mineralogical and chemical interaction between granite and country rock is widespread. Where the granite intrudes calc-silicate rocks, a 'skarn-like' assemblage occurs and the granite is white, consisting of albite clinopyroxene red-brown euhedral sphene. In contrast, where the granite intrudes carbonaceous sediments, particularly in the Kuridala Formation, it is green, and sulphide rather than magnetite becomes the dominant opaque phase.

(3) Regional metasomatic alteration. 'Red Rock' alteration is widespread in both granite and country rock, but appears more common at contacts between high-SiO_2 granite and breccia zones. The alteration products are of two types: either the rocks are high in K_2O and low in Na_2O, or high in Na_2O and low in K_2O (Fig. 17). They also have more elevated Fe_2O_3:FeO ratios than the unaltered granites (Fig. 17). Boundaries between fresh granite and both alteration types are sharp.

Geophysical signatures

High K, Th and U values have given the batholiths a strong radiometric signature, with the more SiO_2-enriched plutons giving the strongest response. However, an ancient regolith (Mesozoic ?) over some parts of the batholiths shows deep chemical leaching of virtually all the K, Th and U, so that the radiometric signature is markedly less. The regolith is well developed over the Gin Creek Granite, which occurs immediately west of the Starra deposit and is one of the most fractionated plutons in the Williams Batholith with high values of K, Th and U. The pluton is not anomalous on the regional airborne radiometrics. This effect is only associated with the ancient regolith, as modern regolith profiles have retained K, Th and U, even where the granite is physically broken down by weathering into individual grains.

The magnetisation of the granite and its surrounding aureole is quite variable. Mafic phases of the batholiths have high magnetic susceptibilities (over 4000 X 10^{-5} SI units), owing to magnetite, thus these granites appear as broad circular magnetic domes. Particu-

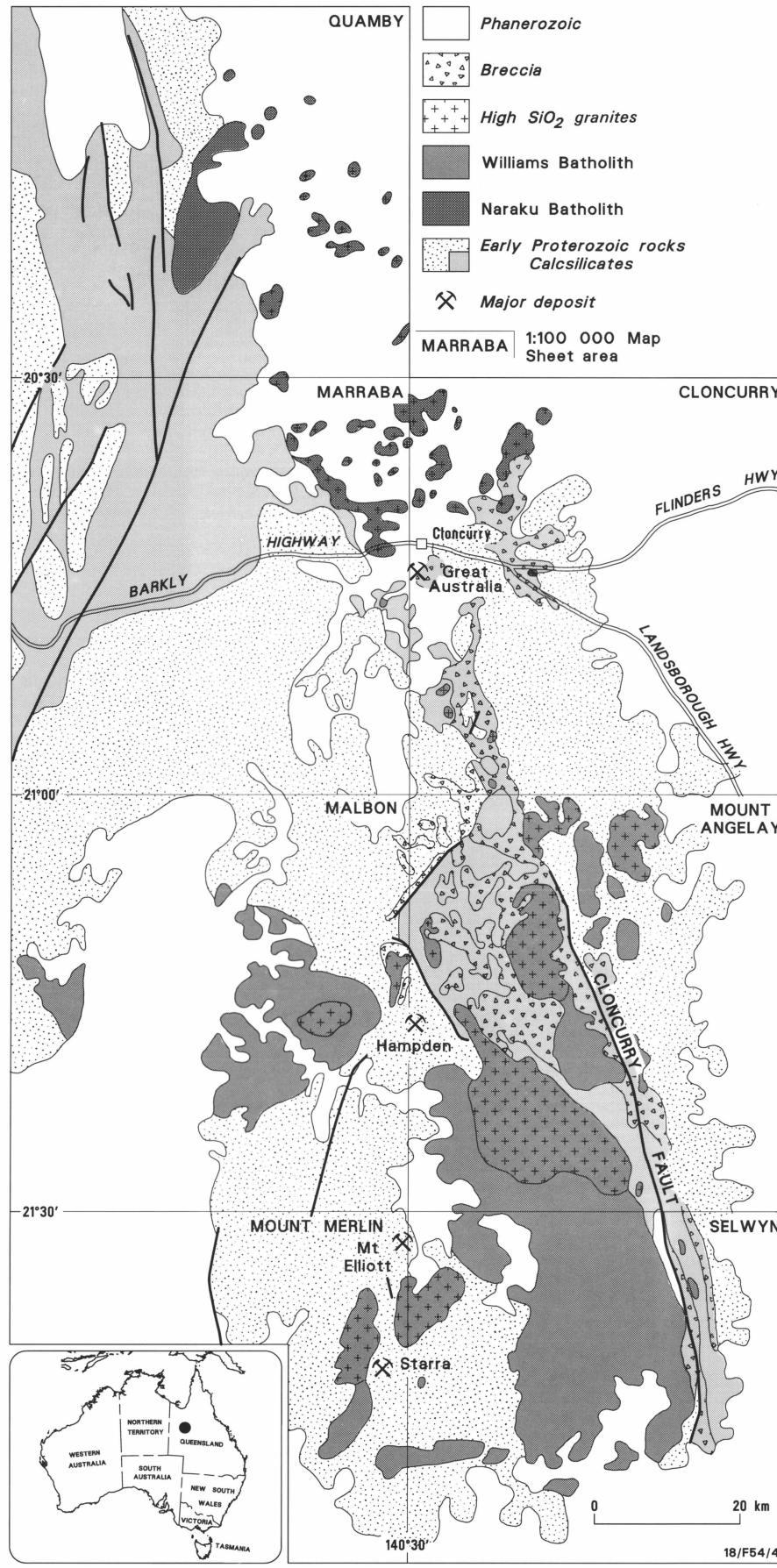

Fig. 16. Distribution of granite in the eastern Mount Isa Inlier. (NB. Breccias have only been distinguished in regional mapping in the Cloncurry, Mount Angelay, and Selwyn 1:100 000 Sheets: they may be more extensive on the remaining map sheets.) Modified from Blake (1987: Geology of the Mount Isa & Environs, Queensland & Northern Territory 1:500 000 scale map. *Bureau of Mineral Resources, Canberra).*

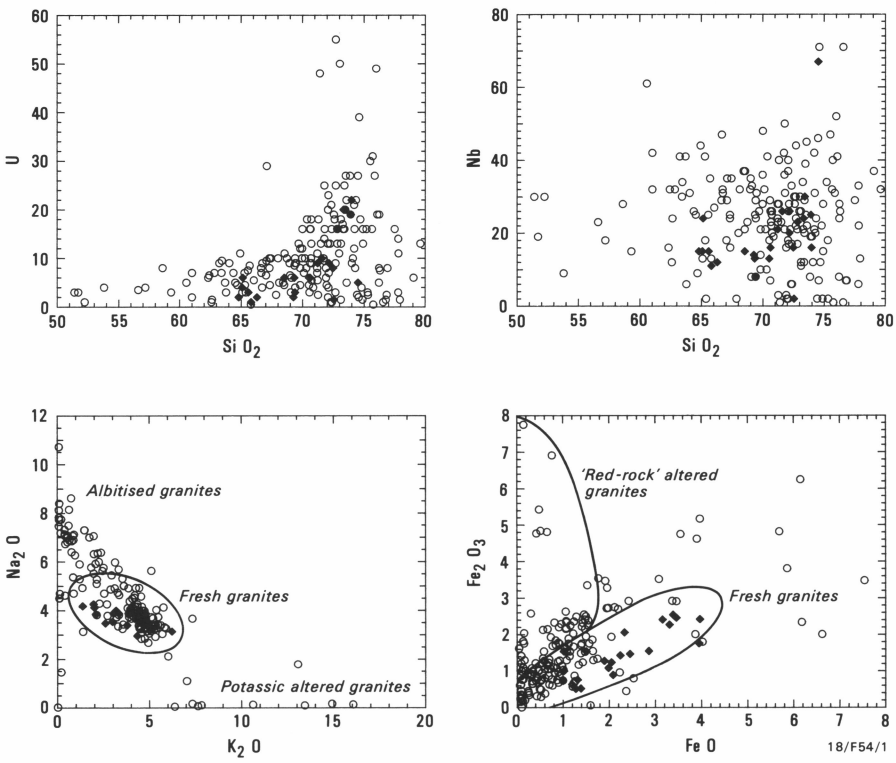

Fig. 17. Chemical variation diagrams for the Williams Batholith (open circles) and Naraku Batholith (filled diamonds).

larly where the granite intrudes calc-silicate rocks, the surrounding aureole can have high magnetic susceptibility; and where the pluton is non-magnetic, the aureole is a circular ring on regional magnetic maps.

Wellman (1990, *BMR Yearbook 1990*, 15) identified six major geophysical domains in the geological formations that crop out in the Mount Isa Inlier, and predicted extensions beneath the Eromanga, Carpentaria and Georgina Basins (Fig. 19). Large circular structures have been recognised from magnetic data in the extensions of those domains intruded by the Williams and Naraku Batholiths, and these are believed to be plutons equivalent to the batholiths beneath the Phanerozoic sediments.

Fig. 18. Compositional variation in the eastern half of the Williams and Naraku Batholiths. Lines indicate the level of erosion on the relevant 1:100 000 Sheet area.

Metallogenic significance.

Small Au, Ag, Cu and U deposits are located within and at the margins of some of the plutons, suggesting a genetic relationship between the two. Laing (1990, *Mount Isa Symposium, Monash University*) noted how deposits, such as Mount Dore, Kuridala, Stuart, and Mount Freda, lie along either D_3 faults, or D_2 mylonitic faults that were reactivated brittly during D_3; he interpreted D_3 as synchronous with the intrusion of the Williams Batholith.

Wyborn & others (1987: *Geological Society of London, Special Publication* 33, 397–394) noted the chemical similarity between the Williams Batholith and the granites of the central Gawler Craton and Stuart Shelf, SA. Hematite breccias in the Williams Batholith are also strikingly comparable to those described at Olympic Dam by Oreskes & Einaudi (1990: Economic Geology, 85, 1–28).

The metallogenic significance of fractionation and magmatically associated brecciation and alteration in the Williams and Naraku Batholiths and surrounding areas cannot be over-emphasised, particularly for Cu and Au.

Fig. 19. Possible subsurface extent of the Williams and Naraku Batholiths based on geophysical data (after Wellman, in prep).

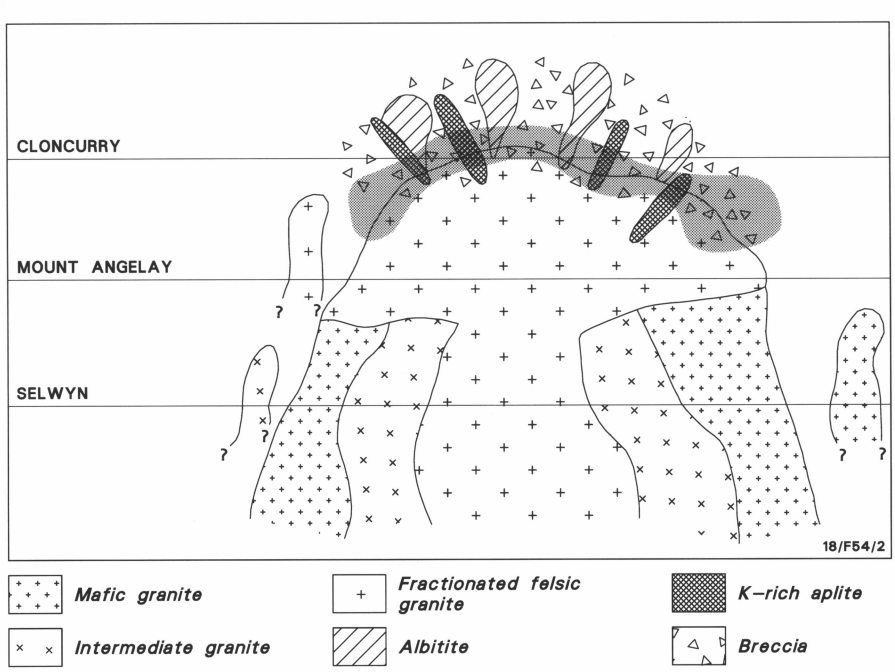

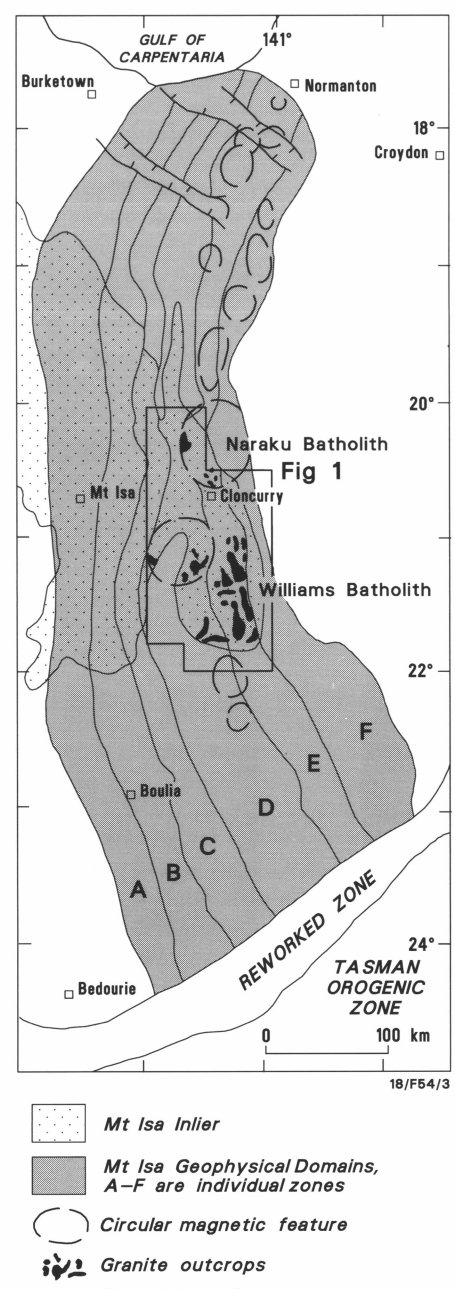

The recent announcement of significant Cu and Au results from a joint venture drilling program by Western Mining Corporation and Hunter Resources near Fort Constantine, 14 km northeast of Cloncurry, demonstrates this forcefully.

For further information, contact Dr Lesley Wyborn (Minerals & Land Use Program) at BMR.

New tectonic model for the Cobar Basin, NSW, points to new exploration targets in Lachlan Fold Belt

In the knowledge that a major deep seismic reflection study was to be undertaken in the Cobar Basin, northern Lachlan Fold Belt (Fig. 20), Glen (1991: *BMR Journal of Australian Geology & Geophysics*, 12, 13-24) described the tectonic evolution of the basin and discussed models of ore genesis from a pre-seismic viewpoint, stating that 'Modifications to these "pre-seismic" models will come as no surprise.' The data from the 1989 ACORP survey have now been interpreted. They show the Cobar Basin to be a cold ramp basin, and not a classical extensional basin.

The basin is asymmetric, with a steeper east-dipping western edge and a more gently dipping eastern edge (Fig. 21). Its maximum depth is approximately 6 km. The section southwest of the basin, on Line C1, has a characteristic seismic signature, showing sedimentary cover rocks dipping gently westwards across a folded Ordovician basement, which in turn overlies more flat-lying rocks. At the western boundary of the basin, these rocks are truncated by the Dusty Tank Fault (Fig. 20), which dips eastwards. Recognition of this signature on Line C3A allowed the western boundary to be mapped farther north, where it corresponds to the Jackermaroo Fault.

On the central line (Line C2), the western margin corresponds to the eastern side of the Nullawarra Anticline, located along strike to the Dusty Creek Fault (Fig. 20). The western edge of the basin is structurally more complex than the other edges, with along-strike variations in position and geometry demanding the presence of tear faults.

The eastern margin of the basin has been defined by surface mapping as a north–south-striking system of linked faults. Bands of reflections with surface projections corresponding to the main fault, the Rookery Fault, were mapped in the seismic data, dipping westward under the basin to intersect its western boundary at about 6 km depth (Fig. 21).

The structural styles within the basin vary with depth. In the top 1–1.5 km, the sediments are folded into synforms and antiforms, which generally correlate with synclines and anticlines mapped in the surface rocks. Intrabasinal folds and faults detach both within and at the base of the basin. Different responses to deformation above and below these detachments indicate that the deformation during inversion was thin-skinned.

The seismic data support a ramp detachment model (Fig. 22), in which the basin formed when the upper crust was moved across the lower crust along a detachment that ramps from about 12–16 km depth in the west to about 25 km depth under the eastern side of the basin. The net displacement of the upper crust, relative to the lower crust (basin opening less basin inversion), was approximately 24 km at an azimuth of 40° east of north. The strike of the ramp in the detachment is west of north, and is not orthogonal to the direction of the net movement vector. In adjusting to the flexure caused by movement across the topography in the detachment, the upper plate fractured along two fault systems. One system comprises the faults parallel to

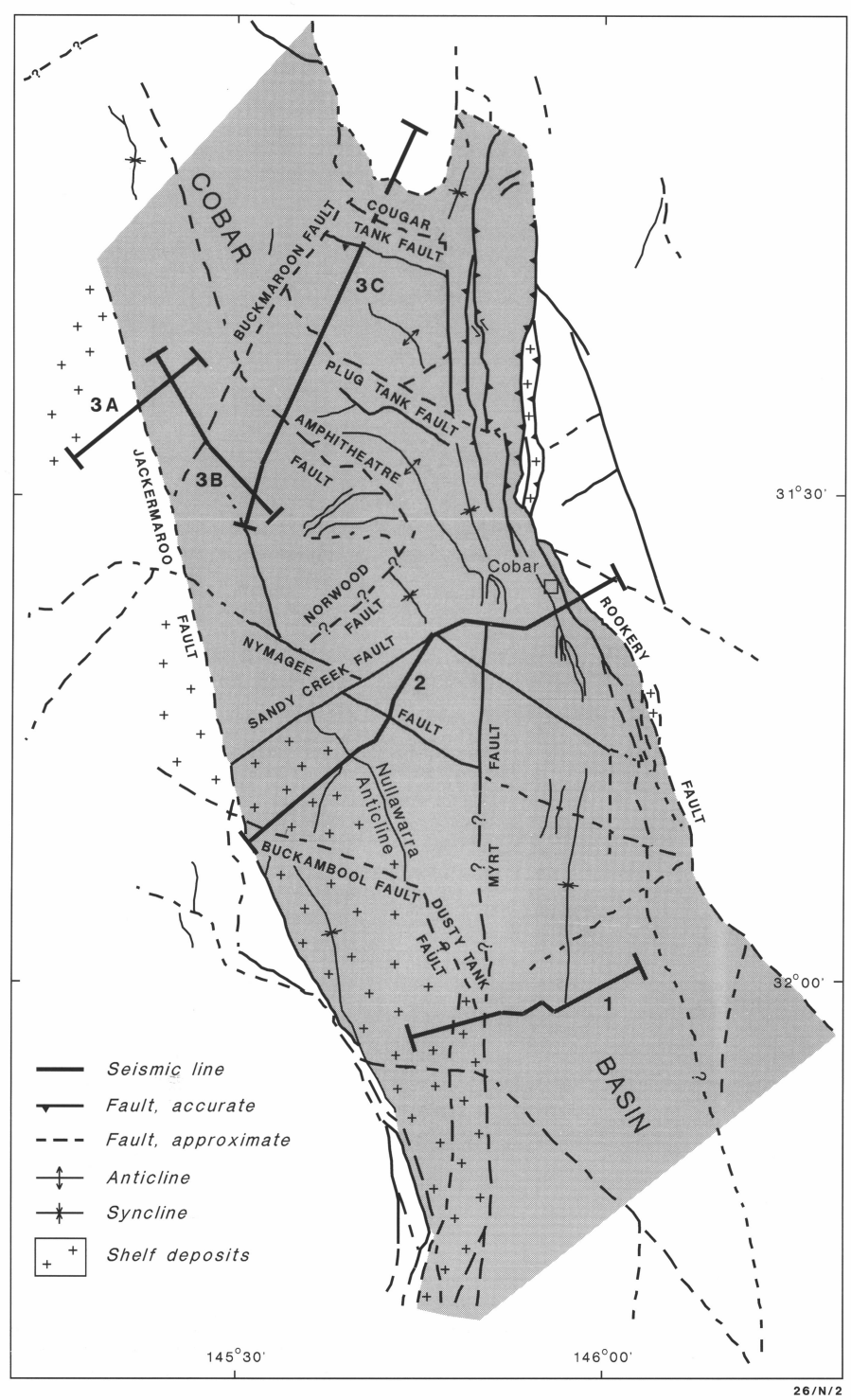

Fig. 20. Location map of the Cobar Basin region, N.S.W., showing structural elements and the location of the seismic traverses (1, 2, 3A, 3B & 3C).

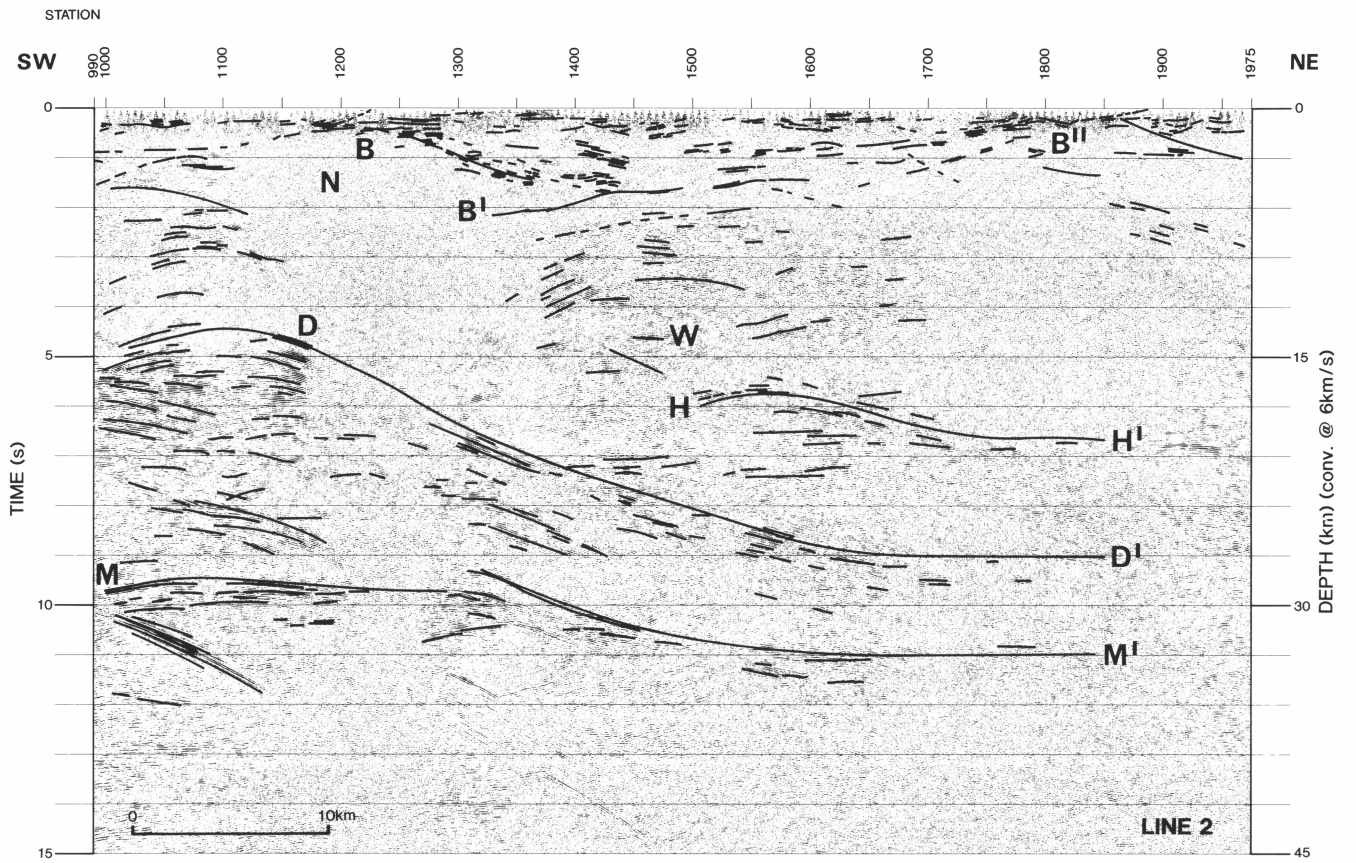

Fig. 21. Interpreted deep-seismic reflection section showing sub-horizontal mid-crustal reflector (H–H'), major mid-crustal detachment (D–D') and crust–mantle boundary (M–M'). 'W' defines a region of weak but continuous mid-crustal fabric. The upper crustal reflectors, defining the major features within the Cobar Basin (B–B'–B"), have been copied from smaller-scale sections. The sub-surface locations of the Nullawarra Anticline (N) is marked.

the western margin of the basin and their associated tear faults. The other comprises faults both parallel and orthogonal to the net movement vector; these faults are confined to the interior of the basin. The linked fault systems provide pathways for migration of fluids during basin formation, late diagenesis and inversion. Faults both within and along basin margins are thus suitable exploration targets. Tear faults along the western margin and within the basin provide additional potential pathways for fluid flow and, therefore, are also exploration targets.

Implications for the Lachlan Orogen

Recent structural/tectonic models for the evolution of the Lachlan Orogen have emphasised the applicability of thin-skinned thrust models (e.g. Glen & others, 1990: *Journal and Proceedings of the Royal Society of New South Wales*, 123, 15–26; Cox & others, 1991: *Australian Journal of Earth Sciences*, 38, 151–170). Most of the evidence has come from Early Silurian and older lithotectonic associations, although some has also come from the Siluro-Devonian Melbourne Trough. Even here, much data come from the eastern side, i.e. in the imbricated older rocks of the Mount Wellington and Mount Easton fault zones.

Glen (1991: *op. cit.*) has suggested that Siluro-Devonian basins of the Lachlan Orogen are also characterised by thin-skinned thrust tectonics. He proposed that blind and emergent thrusts in the Hill End Trough and Ngunawal and Quidong Basins shallow at depth to form part of linked thrust systems, with detachments at the base of, or underlying, the basin being formed by reactivation of extensional fault systems. The imaging of such detachments in the Cobar Basin confirms the applicability of the thrust detachment model to the younger sedimentary basins in the Lachlan Orogen. This, in turn, has implications not only for the tectonic development of the orogen, but also for mineral exploration.

For further information contact Dr Barry Drummond, Dr Bruce Goleby, or Mr Kevin Wake-Dyster at BMR (Onshore Sedimentary and Petroleum Geology); or Dr Richard Glen or Mr Dereke Palmer at the Geological Survey of NSW, Department of Mineral Resources.

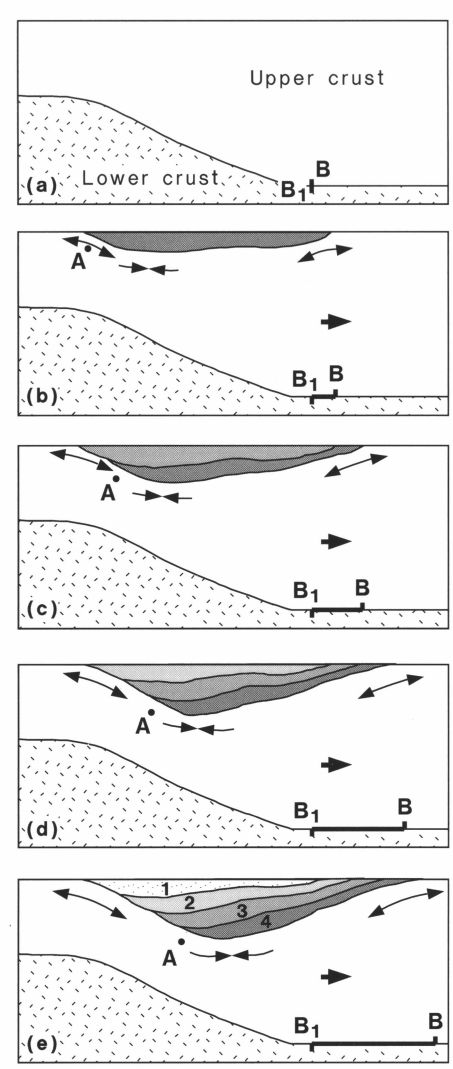

Fig. 22. Ramp detachment model. The basin formed when the upper plate moved to the right across the lower plate. Point A refers to an arbitrary reference point that moves from a tension regime to a compression regime. The points B–B' show the amount of movement within the top plate relative to the bottom plate.

Officer Basin project gets go-ahead

The Officer Basin project was established almost two years ago, in cooperation with the South Australian Department of Mines and Energy as part of the National Geoscience Mapping Accord, to develop a depositional and post-depositional model of the poorly exposed eastern Officer Basin and encourage exploration. To achieve this, BMR plans to carry out a major seismic survey over the central Officer Basin (Fig. 23). The survey grid will cross lands of two Aboriginal communities, the Pitjantjatjara in the north and the Maralinga in the south.

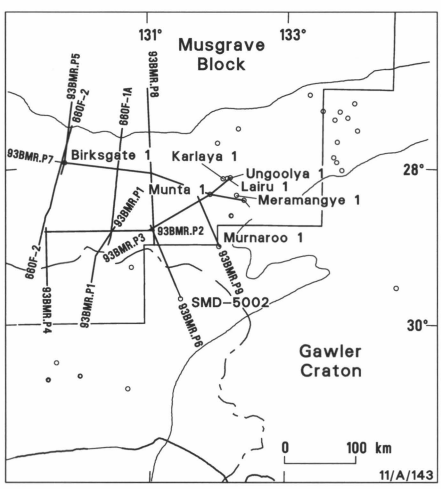

Fig. 23. The eastern Officer Basin, showing possible options for the BMR 1993 seismic survey and location of the 1966 Serpentine Lakes seismic lines now being reprocessed. Solid line – Area of the total magnetic intensity image shown in Fig. 2; Broken line – limit of the onlapping Eucla Basin.

The project has recently taken a significant step forward with an agreement with the Pitjantjatjara Council regarding access to their lands. Agreement in principle with the Maralinga Community was reached in May 1991. These agreements are both important as they allow us to proceed with detailed planning of the survey grid, before final negotiations with the two communities. All being well, the BMR will begin data gathering in Mid-1993.

In the meantime, as plans develop, the Officer Basin team is reassessing existing data. Seismic data covering 7200 km and data from approximately 30 wells are now being reinterpreted with the aim of producing regional structure-contour maps of approximately 13 major sequence boundaries and isopachs of intervening intervals. Simultaneously, analogue vibroseis data gathered in 1966 in the Serpentine Lakes seismic area have been digitised, and are now being reprocessed. Preliminary results of the reinterpretation and reprocessing should become available in late 1992.

Potential field data across the eastern Officer Basin are also being evaluated as a preliminary to basin analysis. Gravity data over the eastern Officer Basin have a denser station coverage than the National Grid, thus providing a good picture of the basin's regional structure. Regional aeromagnetic data were acquired from 1969 to 1982 over most of the Officer Basin by BMR surveys. A total magnetic intensity image (Fig. 24) shows strong east—west lineations in the Musgrave Block, corresponding to both mapped and unmapped faults. Along the northern margin of the basin, the bounding faults vary markedly in character, suggesting that several fault segments are separated by transfer faults.

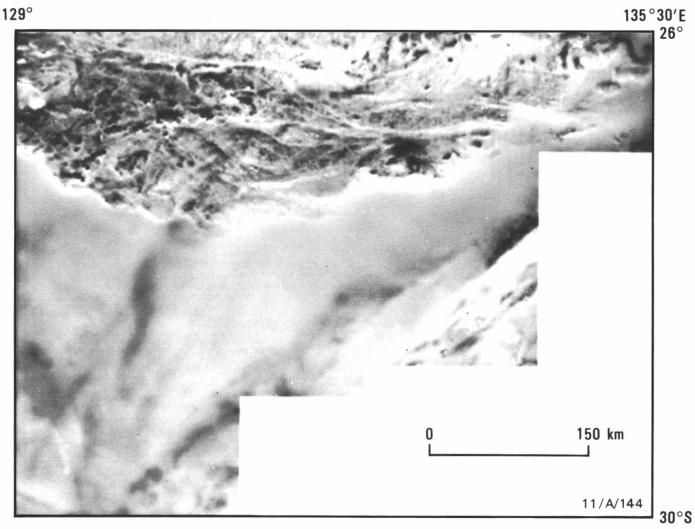

Fig. 24. Total magnetic intensity image of the northern Officer Basin and the Musgrave Block in South Australia. Lineaments outlining known faults and other unknown structures are clearly displayed.

For further information contact Dr John Lindsay or Dr Jim Leven (Onshore Sedimentary and Petroleum Geology Program) at BMR.

Cape York Peninsula update

The strongest argument for a Proterozoic age for the Coen Inlier of far north Queensland has been the apparent continuity of similar rocks between the Georgetown and Coen Inliers. However, recent analysis of the regional gravity and magnetic data reveals a major northwest-trending break in the geometry and magnetic properties of the region (colinear with the northwest-trending portion of the Palmerville Fault Zone, Fig. 25), across which abrupt changes in lithology, metamorphic grade, and structure are inferred. Additional evidence of fundamental differences in the geological histories of the two areas comes from recent ion probe U-Pb zircon dating of granitic and metamorphic rocks, and from new structural data obtained during geological mapping of the Ebagoola 1:250 000 sheet area (EBAGOOLA), Coen Inlier, by BMR and the Queensland Geological Survey (GSQ) in 1991. These data show that the Coen Inlier is characterised by a metamorphic, magmatic and deformational climax of about 400 Ma ago, resulting in complex second-generation structures, amphibolite-grade metamorphism, and voluminous S and I-type granitic magmatism. In contrast, comparable structures, metamorphic assemblages, and S-type granites in the Georgetown Inlier formed 1100 to 1200 Ma earlier. This raises the possibility that the metasedimentary rocks of the Coen Inlier (Fig. 26) are substantially younger than those of the Georgetown Inlier, and may have been derived from them. New high resolution radiometric data have been used to aid regolith mapping at 1:250 000 scale, as well as to distinguish different granite types in areas of poor outcrop and deep weathering. Although broad lithological divisions can be identified in the imagery, most of the variation within these units relates to the regolith cover and to geomorphic processes. Different weathering styles can also be readily discriminated on the imagery. The radiometric imagery can also be interpreted as an 'activity map', identifying stable landforms with deep weathering as opposed to younger landforms with active erosion and stripping of the surficial cover. The imagery thus has considerable potential for guiding interpretation of stream-sediment geochemical data, and for environmental and soil studies as it can delineate areas of erosion and land degradation. Mapping shows that the regolith over most of EBAGOOLA is in situ weathered bedrock. Transported material covers only a small

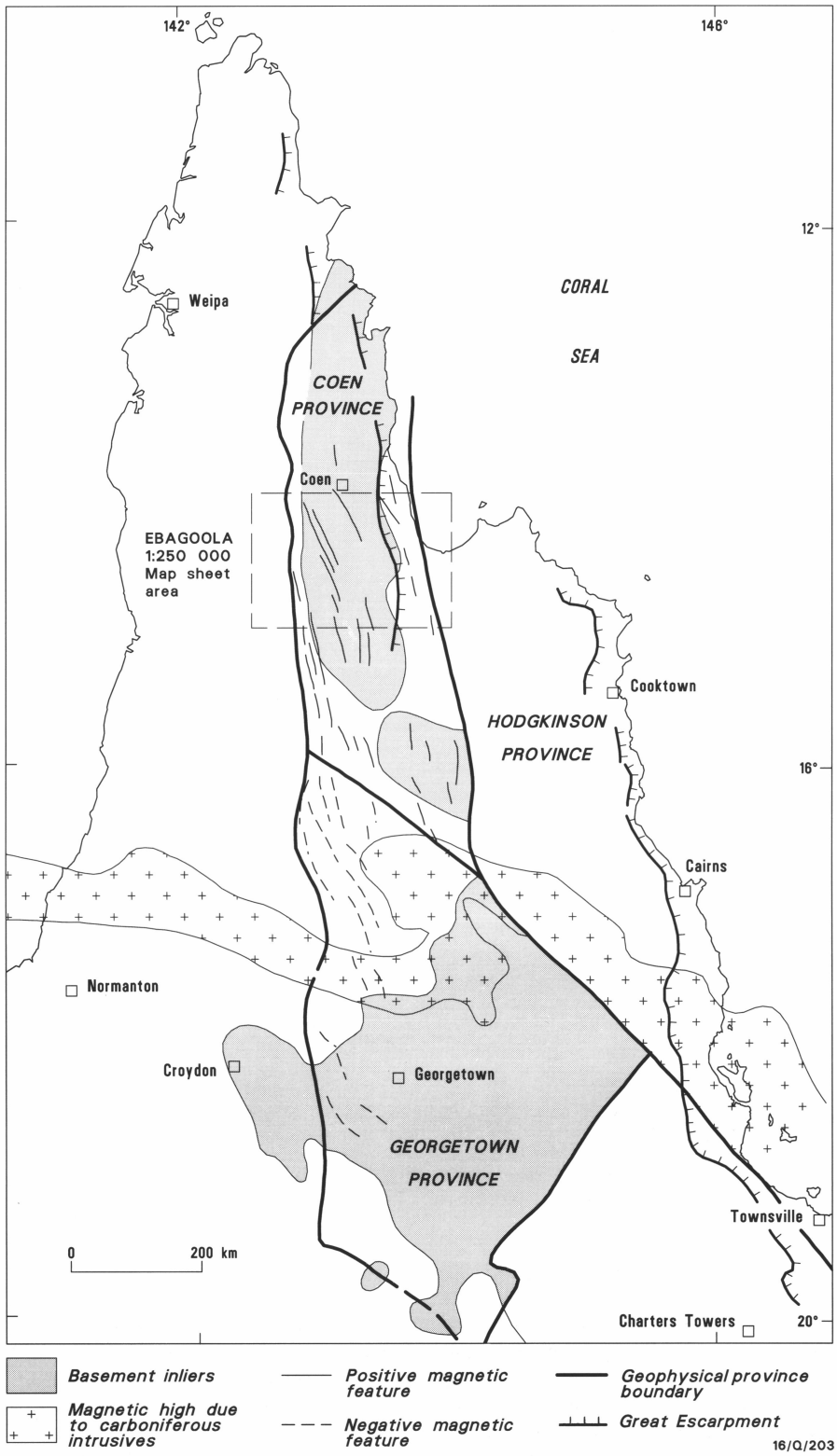

Fig. 25. North Queensland Project area.

part of the sheet area. Regolith distribution closely reflects the geomorphic history, which, in contrast to previous ideas, appears to be one of continual denudation since the end of the Cretaceous. Most activity, and therefore the youngest regolith, is east of the Great Escarpment (Fig. 29).

In the Ebagoola 1:250 000 sheet area (EBAGOOLA), gravity (11 km stations) and magnetic data (400 m line spacing) show that basement east and west of the Coen Inlier comprises meridional bodies of granite and metamorphics similar to those exposed in the inlier (Fig. 27). The belt on the western margin of EBAGOOLA (Fig. 27, 1) is non-magnetic and contains Carboniferous(?) intrusions and volcanics, but is otherwise unknown, as it is completely concealed by Carpentaria Basin sediments.

The central belt of Holroyd Metamorphics (Fig. 27, 2) has, in its central portion, greenschist facies slate, sandstone, phyllite and greenstone, with a relatively simple, folded structure. The eastern and western margins of this belt are quartzite, schist and gneiss with grades as high as upper-amphibolite facies.

Abrupt changes of metamorphic grade occur across major NNW-striking faults. Granite dips under the metamorphic belt on both sides, and is extensive at shallow depth in the north and south of the sheet area, mostly where metamorphic grade is highest. This is consistent with field, structural, petrographic, and geochronological evidence that the metamorphic maximum coincided with the generation and emplacement of the granites.

The eastern metamorphic belt (Fig. 27, 3), consisting of Coen Metamorphics of generally upper amphibolite facies, is not underlain by granite except locally in the north.

Structural geology

In EBAGOOLA, structures associated with the first regional deformation (D1) are widespread in the metamorphic units, and are older than the Cape York Peninsula Batholith (CYPB). In the lower-grade and least-deformed units to the west they are tight to isoclinal, variably plunging first-generation (F1) folds with an axial planar slaty cleavage (S1). In the higher-grade units farther east, intense transposition during the second defor-

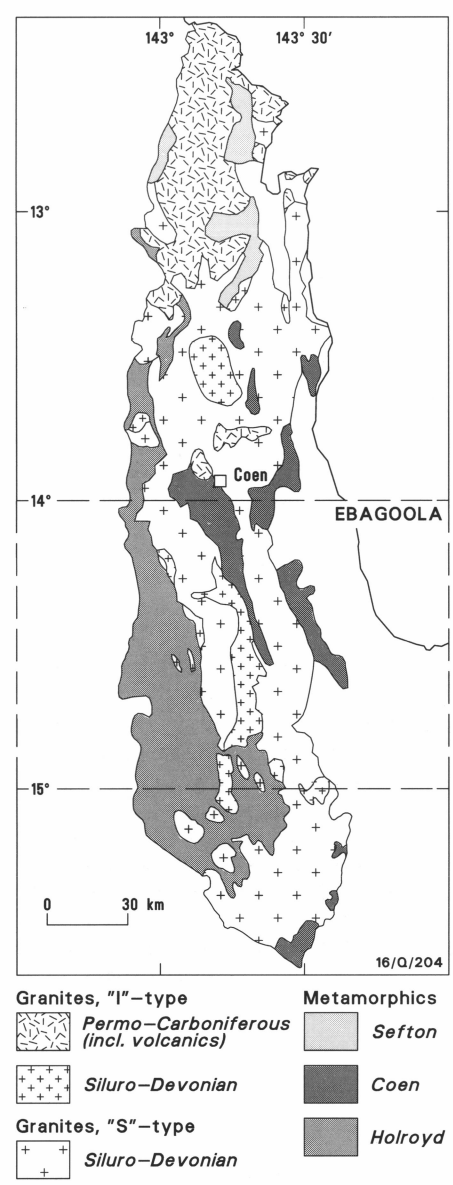

Fig. 26. Coen Inlier.

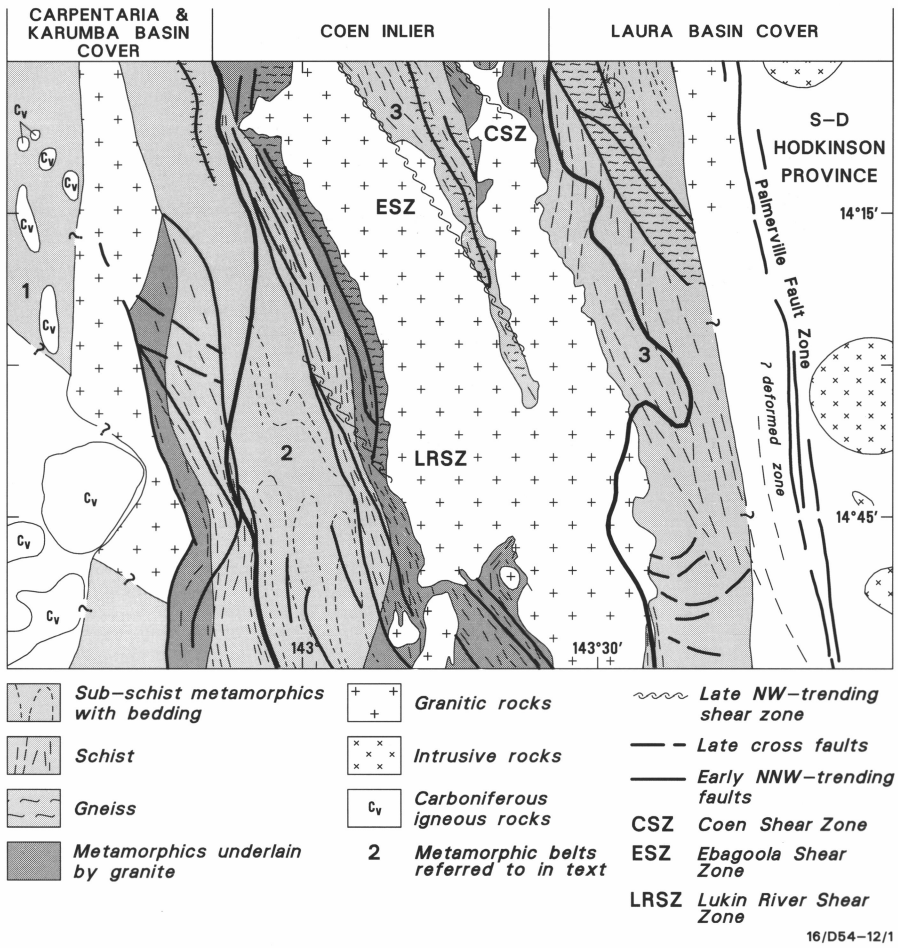

Fig. 27. Main structural elements of EBAGOOLA.

mation (D2) tends to have obliterated most D1 structures.

The first regional metamorphism (M1) may have been a greenschist facies event associated with D1. D1 structures were probably upright and E–W trending (as seen by D1 enveloping surfaces); the age of deformation and associated metamorphism can at present be placed only sometime before about 400 Ma.

The abundant NNW-trending, steeply dipping D2 structures dominate the fabric of the outcropping metamorphics, and define the principal orogenic event in the Coen Inlier. D2 structures consist of subhorizontal to gently plunging isoclinal folds with an axial-plane schistosity (S2, Fig. 28A+B). Most folds are mesoscopic, although macroscopic F2 folds with kilometre-scale wavelengths are present in the south and west. The S2 foliation is commonly seen either as penetrative schistosity with rare gently plunging lineations, or as an intense crenulation foliation with preserved S1 closures (Fig. 28B).

Metamorphism was prograde to upper amphibolite facies, and was associated with the emplacement of the CYPB—this is demonstrated by the continuum between leucosomes in migmatite zones in the Holroyd Metamorphics and a leucocratic component of the CYPB. This provides an approximate 400 Ma age for D2. The latest granite emplacement postdates D2 structures, so the D2 event must be syn-CYPB, or earlier.

Sub-parallel to, but overprinting, the D2 structures are a number of major ductile shear zones, which have important links with gold mineralisation—most quartz-vein deposits of the Coen and Hamilton goldfields lie within or close to the Coen and Ebagoola Shear Zones (CSZ and ESZ; Fig. 27). These NNW-trending shear zones roughly coincide with the granite–metamorphics contacts of the central pendant of the Coen Metamorphics (Fig. 26 & 28E,F) in the CYPB. Shear sense in the mylonites is sinistral, west block up (Fig. 28C), along stretching lineations plunging at 65°. The Lukin River Shear Zone (LRSZ; Fig. 27) is an anastomosing complex up to 10 km wide, separating the low and high-grade units in the Holroyd Metamorphics. Shear sense is consistently sinistral (Fig. 28C) oblique-slip with top to the NNW. Individual mylonite zones are up to 1 km wide.

D3 structures are widespread and include mesoscopic folding and crenulation of earlier fabrics. F3 folds are tight, trend N–S, and plunge steeply (Fig. 28D,E). D3 structures overprint mylonites of the major shear zones, suggesting that D3 is also younger than the CYPB at about 400 Ma.

D4 structures are NE to E-trending folds with weak crenulation foliations (Fig. 28F); kink bands in the more argillaceous units are also thought to be D4.

Geochemistry and geochronology

The first comprehensive study of the Coen Inlier (Willmott & others, 1973: *BMR Bulletin* 135) *identified seven units in the middle Palaeozoic CYPB*[1], and two volcanic and three granitoid units interpreted as late Palaeozoic. Most of these have been resampled[2], and the three CYPB units recognised in EBAGOOLA (Kintore and Lankelly Adamellites, Flyspeck Granodiorite) have been subdivided, and their distribution and relationships reassessed. The Flyspeck suite consists of three or four units and is intruded by the Kintore suite, comprising four units; the Lankelly "Adamellite" (Granite) may be a textural variant of one of the Kintore units.

Most of the Middle Palaeozoic granites show evidence of deformation, ranging from a weak foliation to intense mylonitisation.

Both I- and S-type granitoids are present: the Siluro-Devonian rocks are muscovite–biotite S-type granites (including the Kintore suite) and allanite titanite hornblende-bearing I-type granitoids (including the Flyspeck suite). The Permo-Carboniferous granitic rocks are all I-types.

SiO_2 content of the I-type granitic rocks ranges from about 55 to 77%; whereas the S-types have a more restricted range, about 63–74%, probably reflecting silica-rich sedimentary source rocks. Crystal fractionation was significant in the evolution of rocks with more than 73% SiO_2, as shown by higher K_2O, Ba, Rb and U in these rocks. In particular, the more evolved Siluro-Devonian and Permo-Carboniferous granites are enriched in U, compared with the crustal average[3].

The Siluro-Devonian granitoids have initial εNd values significantly lower (-10.8 to -14.7) than the Permo-Carboniferous I-type granites in the Cape Weymouth area (-6.6 to -7.5); the highly fractionated Twin Humps I-type granite in the Coen area (Fig. 25) has an intermediate εNd value (-8.4). εNd values for the Siluro-Devonian I-type granitoids are mostly lower (-11) than those of the coeval S-type granites (-14). Possibly superimposed on these trends is an increase in εNd from east to west and from south to north. It therefore seems likely that εNd will be useful for delineating and redefining individual plutons.

[1] Whitaker & Willmott (1969: *Queensland Government Mining Journal*, 70, 130–142) restricted the term Cape York Peninsula Batholith to include only granitic rocks of Devonian age. However, we here use the term 'batholith' to define a granitic structural entity with no age connotations.

[2] U-Pb zircon age and Nd isotopic determinations have been carried out on eleven samples collected by R. J. Bultitude (GSQ) during an independent reconnaissance of the Coen Inlier in 1989, as part of the GSQ Hodgkinson Province project. An additional 13 samples have been analysed for Nd isotopic compositions, and 82 samples collected in 1990 have been studied petrographically and analysed for a full range of major and minor elements.

[3] 2.8 ppm; Taylor & McLennan, 1985: *The Continental Crust: Its Composition and Evolution*, Blackwell.

K-Ar and Rb-Sr dating of Cape York granites by Cooper & others (1975, *Journal of the Geological Society of Australia* 22, 285–310), carried out at the time of the original mapping, indicated four periods of Palaeozoic igneous activity, at about 415 Ma, 400 Ma, 390–385 Ma, and 280–255 Ma. Until the current study, the significance of the ages about 400 Ma was uncertain, mainly because demonstrably Precambrian rocks from the Georgetown Inlier (some of which were considered equivalent to granites in the Coen Inlier) had also given Rb-Sr and K-Ar ages of about 400 Ma.

Recent U-Pb zircon dating of granitic rocks in the Coen Inlier of Cape York (Fig. 2), using the SHRIMP ion microprobe at the Australian National University, has confirmed the Siluro-Devonian (ca. 408 Ma) and Permo-Carboniferous (ca. 284 Ma) ages of the I-type and S-type granitic suites making up the CYPB. Granitic rocks of unequivocal Proterozoic age have not been identified, although Precambrian zircons, mostly about 1600 Ma, but ranging up to 2500 Ma, are common in many of the granites.

The U-Pb zircon data and Sr and Nd isotopic compositions of the CYPB granitoids can be interpreted in terms of the same two major source components (c. 1600 and 2100–2500 Ma) deduced by Black & McCulloch (1990: *Geochimica et Cosmochimica Acta*, 54, 183–196) to have been involved in the generation of the Siluro-Devonian granitoids of the Georgetown Inlier. An important difference is the absence of S-type granites of this age in the Georgetown Inlier, whereas they dominate the Coen Inlier. The Late Palaeozoic I-type igneous rocks in both regions are sufficiently similar in initial Nd isotopic composition to have been mostly, if not totally, derived from comparable 1600 Ma source rocks.

A major difference between the Georgetown and Coen Inliers is the absence of positively identified *Precambrian* igneous rocks in the latter. Furthermore, despite the similarities between the two regions noted above, there is no unequivocal indication that the metasedimentary units (Holroyd Metamorphics, Sefton Metamorphics and Coen Metamorphics) of the Coen Inlier *are* Precambrian. A single age for the Coen Metamorphics indicates a *source* about 1550 Ma old, but does not confirm a Proterozoic *depositional* age. It is, thus, possible that the metasedimentary units of the Coen Inlier are composed of relatively young rocks (e.g. Late Precambrian–Early Palaeozoic) that were derived from an old terrane, such as the Georgetown Inlier.

Regolith

New high-resolution airborne radiometric data (400 m line spacing) for EBAGOOLA has proved invaluable for differentiating regolith types, based on their potassium (Fig. 29), thorium and uranium signatures, partly because the radiometric signal, unlike Landsat TM, effectively 'sees through' the vegetation cover and as much as 40 cm below the surface.

Most regolith mapping depends on landforms to place regolith unit boundaries. However, where landform boundaries are not continuous, the radiometrics allow boundaries to be completed. They also allow much more confident extrapolation of field results to areas not visited.

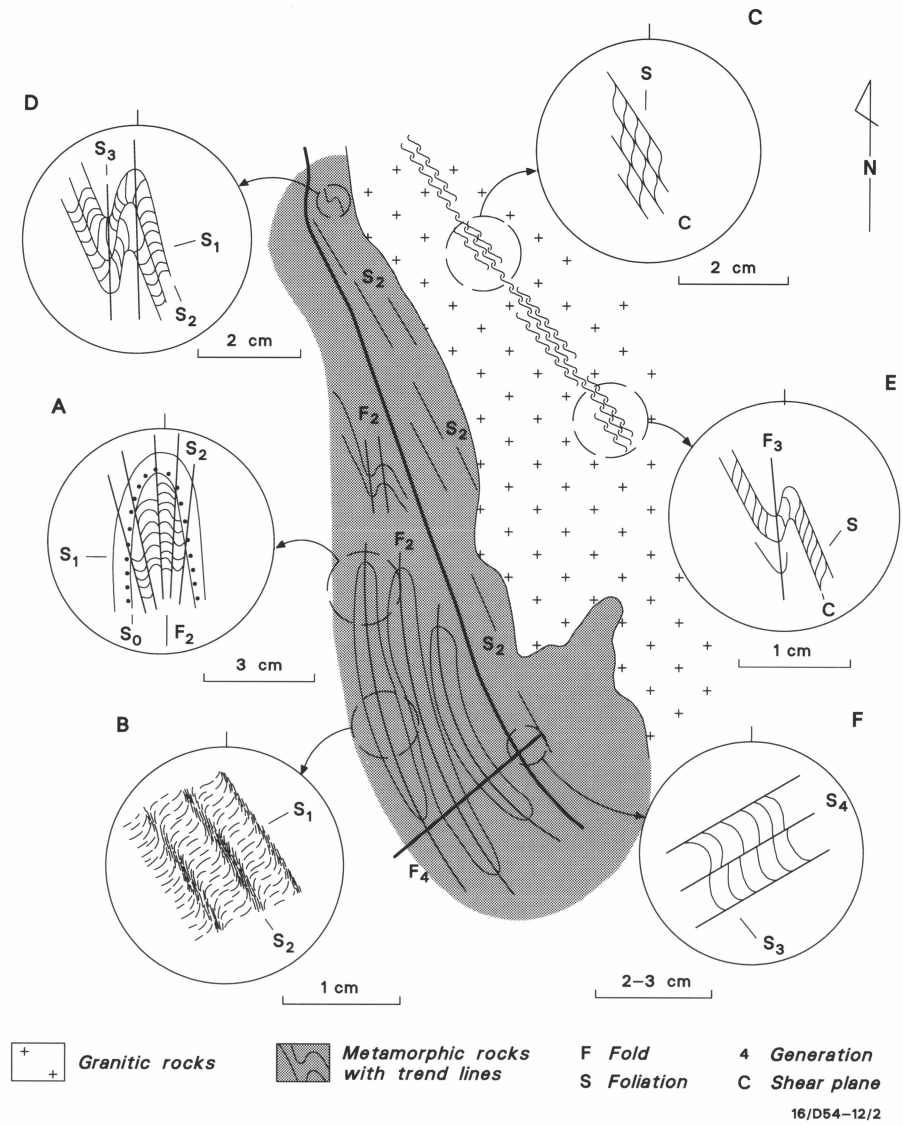

Fig. 28. Schematic fabric element sketch for EBAGOOLA.

Radiometric response of regolith materials differs with bedrock type. Within areas of homogeneous bedrock, radiometric signatures can be used with confidence to map regolith types in some detail. Equally important, the radiometrics give a clear indication of the geomorphic environment, and may be used to assess the degree of relative 'geomorphic activity'.

EBAGOOLA can be divided into three broad physiographic provinces (Fig. 29):

(1) The **eastern coastal plain** is dominated by depositional processes. Sediments derived from granitic and metamorphic rocks of the central uplands form broad alluvial outwash fans and braided-stream deposits. Along the east coast, they have been reworked by tidal and wave action and deposited as beach ridges and chenier plains. The distribution and origin of these sediments is recorded in the imagery by high potassium and thorium signatures, reflecting, respectively, granitic and metamorphic source rocks.

(2) The **central uplands** are essentially an erosional landform. Material is being removed by rivers draining both east and west, flowing, respectively, into Princess Charlotte Bay and the Gulf of Carpentaria. Deep residual sands over mottled and pallid zones characterise the granitic terrains, and reflect *in situ* chemical weathering. They are recognised by very low radiometric counts in all three bands.

Areas of active stripping on granite have high potassium counts, reflecting the high feldspathic content. Erosional scarps form broad scallop patterns on the imagery. On metamorphic rocks, high radiometric values are also found on steep, more active slopes, while areas with lower response reflect the lower-angle quartz-rich regolith in valleys.

(3) The **western plains** contain many palaeoforms, and have experienced a long history of weathering with at least one cycle of drainage inversion. Low potassium and relatively high thorium counts in this province are associated with deeply weathered sandy soils. Moderately high potassium values over the northwest corner of EBAGOOLA correspond to cracking clay soils, and perhaps reflect the presence of potassic clays (i.e. illite) and/or absorption of potassium ions within

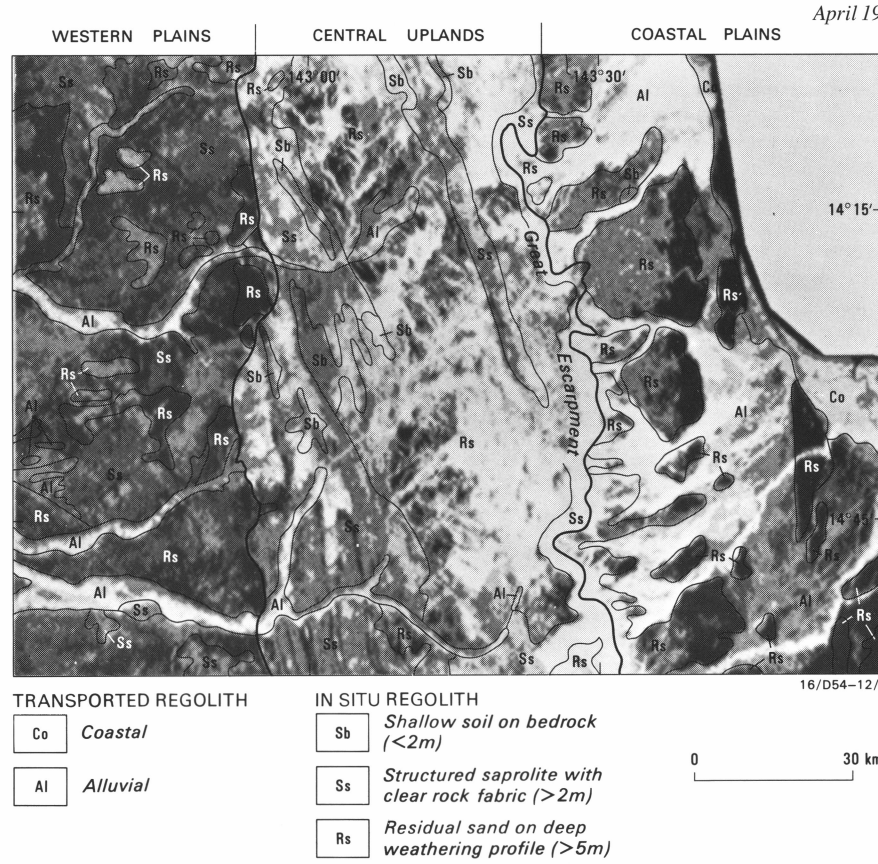

Fig. 29. Dominant regolith types superimposed on a grey-scale image of the potassium channel radiometrics, EBAGOOLA.

the lattice of swelling clays (i.e. montmorillonite).

Deeply weathered residual plateaus surfaced by bauxitic or ferruginous pisolitic material are recognised by their high thorium signatures, probably reflecting resistant minerals, such as zircon, rutile, and monazite.

Rivers flowing from the central uplands are clearly seen in the imagery, as they reflect the high feldspathic content of the alluvium. Channel and overbank deposits may be distinguished, the latter being relatively less bright than the former.

For further information contact Project Manager (BMR), John Bain (06 249 9282); Geochronologist, Lance Black; Structural geologist, Richard Blewett; Petrologists, Bob Bultitude (GSQ), Jan Knutson, Doug Mackenzie; Regolith geologists, Colin Pain, John Wilford, John Dohrenwend (USGS); Isotope chemist, Shen Su Sun; Metamorphic geologists, David Trail, Friedrich von Gnielinski (GSQ); Geophysicist, Peter Wellman.

Mapping in high-grade terranes: use of remotely sensed data and airborne geophysics

Regional mapping in the high-grade metamorphic terranes of the Arunta and Musgrave Blocks of central Australia by BMR and the Northern Territory Geological Survey highlights the problem of scale. The penetrative deformation and recrystallisation associated with high-grade metamorphism have transformed many of the original rock units into packages of interdigitated small-scale units, obliterating original geological boundaries and resulting in imperceptible transitions between distinct lithological assemblages.

Partial melting, remobilisation and anatectic injection of veins, bands and migmatite units occur on a range of scales. Interpolation of field data aimed at defining macroscale map units may thus be complicated, despite many field traverses and petrographic examinations. In many instances, distinct lithological marker units facilitate the field mapping, e.g. basic granulite units in Redbank Hill, west Arunta Block, whereas elsewhere consistent markers may be difficult to define, e.g. Mount Aloysius massif, Tomkinson Ranges, western Musgrave Block, where granulite-facies layered felsic supracrustal rocks include lenses and schlieren of basic to intermediate granulites.

In some instances, the charting of macroscale units is helped by colour aerial photography manifesting the effects of minor lithological variations, weathering and vegetation. However, interpolation between geological traverses conducted, for example, along well-exposed creeks, is commonly complicated by intervening unexposed or rubbly terrains.

The role of airborne magnetic and radiometric data and other remotely sensed data has, therefore, been considered in relation to the identification of macroscale units and interpolation across unexposed terrain.

Airborne geophysical techniques

The strengths and weaknesses of each method have been assessed: total magnetic intensity maps enable demarcation of major structures and magnetically distinct units, e.g. along both the Redbank–Mount Zeil thrust zone in the western Arunta Block, and the Hinckley and Mann faults in the Musgrave Block. Mutton & Shaw (1979: *Bulletin of the Australian Society of Exploration Geophysicists*, 10, 79–91) have correlated airborne total magnetic intensity data with induced magnetic susceptibility and remanent magnetic intensity from ground and sample data, in relation to the composition of granulite facies gneisses in the western Arunta Block. They showed that the magnetic properties depend on rock composition only in a general sense, and are otherwise affected by total iron content, oxygen fugacity of the rocks, the temperature-dependent history of remagnetisation, and degree of metamorphism.

Thus, the magnetic properties and the parameters used to classify rock types may not be directly related. Since the magnetic properties of mappable units may vary in different areas, interpretation of magnetic anomalies must be coupled with ground and laboratory data on magnetic susceptibility and remanent components.

Airborne gamma-ray data on potassium, uranium and thorium may represent either their primary concentrations or their secondary redistribution patterns, noting the high mobility of uranium and the relative mobility of potassium under hydrous conditions. The common depletion in radiogenic elements in some high-grade metamorphic terranes has been attributed to low-degree partial melting and/or loss of a volatile phases enriched in these elements (Lambert & Heier, 1968: *Lithos*, 1, 30-53). Thus, whereas in some terranes the radiometric data delineate contrasting lithologies, in others they reflect metamorphic redistribution patterns which bear little or no relationship to lithologically distinct map units. Resolution of these uncertainties requires geochemical testing of the significance of radiometric anomalies.

Remotely sensed data

Remotely sensed data in the visible and near-infrared (VNIR: 0.40–1.0 μ m), shortwave infrared (SWIR: 1.0–3.0 μ m), and midthermal infrared (MIR: 8.0–14.0 μ m) band ranges correlate with characteristic features of a wide range of minerals and lithologies, owing to the absorption, reflection or emission features arising from electronic changes in transition elements, bending/stretching vibrations in hydroxyl-bearing phases and carbonates, and Si–O vibrations in silicates. Thus, the identification of sheet-structured

hydrosilicates, amphiboles, epidote, quartz, rare-earth-bearing minerals, carbonates, and iron oxides allows effective discrimination of the alteration products of primary rock types. Consequently, the dominance of hydrosilicates in greenschist and amphibolite facies terranes allows their remotely sensed identification to a greater extent than in dehydrated igneous and granulite facies terranes.

BMR's studies of layered basic and ultrabasic intrusions in the Pilbara Block, Western Australia, have been greatly assisted by remote sensing of characteristic alteration and weathering products (Simpson & Macias, 1987: *Proceedings of the 4th Australasian Remote Sensing Conference*, 364–370). This work requires careful identification and consideration of weathering, vegetation, and fireburn effects (Simpson, 1990: *Journal of Remote Sensing*, 11, 2019–2034). In some cases, recent fireburns provide little-obscured bedrock 'windows', e.g. in the central Pilbara region, using Geoscan Mark-I imagery, which may be extrapolated once vegetation-screening techniques are established for different geographic/climatic regions. The vegetation cover (especially spinifex), combined with the scarcity of hydrosilicates in granulite-facies rocks, requires that the use of remotely sensed imagery in high-grade terranes must often rely on identification of characteristic alteration products.

In the basic-ultrabasic Giles Complex and its high-grade felsic metamorphic and igneous host rocks in the Tomkinson Ranges, Thematic Mapper (30 m pixel) and Geoscan Mark-I (10 m pixel) imagery effectively correlates with surficial deposits, including calcareous and ferruginous duricrusts, and a range of detrital materials (Feeken, 1991: *BMR Research Newsletter*, 14, 7–8). By contrast, only broad distinctions are observed between basic, ultrabasic, and felsic metamorphic and igneous units. Given the scale problems, the interpretation of data acquired by high-resolution multi-band scanners potentially offers rapid and accurate recognition of cryptic macroscale units in exposed and thin gravel-veneered terranes.

Conclusions

No single method can provide a panacea for mapping high-grade terranes and a *combination* of field, airborne geophysical, and, most notably, multispectral remotely sensed data is required to map units accurately on a regional scale. In the future, multispectral satellite imagery, including mid-thermal infrared (MIR) emission data, offers the potential for analysis and integration of reflection/absorption and emission spectra, applying vegetation-screening methods and multicomponent unmixing analysis (Bierwirth, 1990: *International Journal of Remote Sensing*, 11, 1999–2017). This should allow the resolution of diagnostic criteria for lithological identification and production of a new generation of detailed maps under the National Geological Mapping Accord.

For further information contact Dr A.Y. Glikson or Dr A.J. Stewart, Minerals and Land Use Program, BMR.

BMR detects hydrocarbon pollution off Sydney

Geochemical equipment on BMR's *RV Rig Seismic*, designed to detect seepage of petroleum hydrocarbons from sub-seafloor accumulations into the bottom-waters of the Australian continental shelf, recently demonstrated its potential for environmental monitoring in a novel pilot survey with the Sydney Water Board (SWB). The survey was undertaken to test the continuous geochemical profiling equipment aboard *Rig Seismic* for use in environmental geochemistry and oceanography. High concentrations of light (C_1–C_6) hydrocarbons were measured in seawater off Sydney, indicating anthropogenic (man-made) additions to the coastal zone. The hydrocarbons appear to emanate from Botany Bay, the inner part of Port Jackson, and the SWB ocean outfall sites located at Malabar, Bondi and North Head. The ratios of various light hydrocarbons in the plumes provide one approach to delineate potential sources of hydrocarbons.

The equipment (previously described in *BMR Research Newsletter*, 10, 12–13, 1989) consists of a tow-fish from which seawater is continuously pumped into the geochemical laboratory aboard *Rig Seismic*. Light (C_1–C_8) hydrocarbons are continuously extracted from the seawater and analysed by gas chromatography. Total volatile hydrocarbons (THC) are measured every 30 seconds, C_1–C_6 every two minutes, and C_5–C_8 every eight minutes. At a ship speed of 5 knots, C_1–C_6 concentration-data are collected each 300 m of seafloor traversed, and continuously displayed in the ship laboratory and stored on a PC for subsequent processing and analysis. Hydrographic data (temperature and salinity), the altitude of the tow-fish above the seafloor, and the depth of the tow-fish in the water column are also continuously displayed and recorded.

The survey collected data over approximately 60 km from the vicinities of the entrance to Botany Bay, and the SWB ocean outfall sites at Malabar, Bondi and North Head, including a transit line into Port Jackson as far as Fort Denison. Also included was a vertical profile, in about 80 m water depth, south of the Malabar ocean outfall site and off the entrance to Botany Bay.

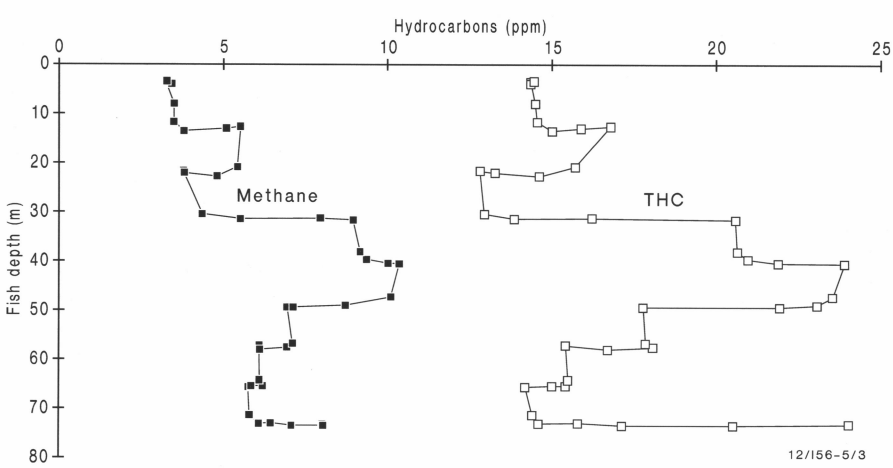

Fig. 30. Vertical profiles of total volatile hydrocarbons (THC) and methane in seawater from off the entrance to Botany Bay and south of the SWB ocean outfall site at Malabar.

The vertical profile (Fig. 30), carried out at the beginning of the survey, shows methane and total volatile hydrocarbon (THC) maxima between 30 and 50 m water depth; hence the tow-fish was set at about 40 m for most of the remainder of the survey. The methane and THC concentrations measured in the mid-water plume were all significantly (two-to-three-fold) higher than typical background values, suggesting anthropogenic sources for the hydrocarbons. High concentrations of hydrocarbons in the bottom-waters (>70 m water depth) suggest input from the sediments. The depth of the plume in the water column is probably controlled by a dynamic balance between the buoyancy of the plume and the density stratification (vertical profiles of temperature and salinity). Because the temperature and salinity (hence stratification) of the ocean waters vary seasonally, the depth and dispersion of the plume would be expected to vary also throughout the year.

The distribution of light hydrocarbons (at 45 m water depth) in seawater along the coastal transect is summarised in Figure 31. Total volatile hydrocarbons (THC) and methane (Fig. 31A) are at background levels in the most southern part of the survey area, rapidly increasing towards the entrance to Botany Bay. The highest concentrations of THC and methane were found near the SWB ocean outfall sites at Malabar, Bondi and North Heads. Methane was about ten times background near the outfall sites.

From the limited data, these plumes could be detected about 5 km alongshore from the outfalls. Select C_{2+} hydrocarbons (ethane, propane and butane) are summarised in Figure 31B, and show distribution different from those of THC and methane. The highest concentrations (more than ten times background)

of propane and butane were found in the southern sector of the survey, near the entrance to Botany Bay and south of the outfall site off Malabar, while minor amounts of ethane (about twice background) were associated with the entrance of Botany Bay and the outfall sites off Malabar, Bondi and North Head. During the transit along Sydney Harbour, the highest concentrations of C_{2+} hydrocarbons were found toward the 'inner' harbour, as Fort Denison was approached.

Hydrocarbons added to seawater are rapidly dispersed by mixing, so that their lateral distribution may not be a unique indicator of their source. To further investigate source, a variety of cross-plots of the hydrocarbon compositions in the plumes may be used. A cross-plot of ethane vs. propane for all data collected during the survey (Fig 32) shows the data falling into three sectors: a coastal transect, the vertical profile (off Botany Bay), and the Sydney Harbour transit. Typical backgrounds plot to the left origin, while trends to higher concentrations plot away from the background, reflecting the different potential sources of hydrocarbons contributing to the anomalies.

In the plot, two types of hydrocarbon source with different ethane/propane ratios can be identified. (1) A trend of increasing ethane concentration with minor propane increase includes data from the coastal transect (Botany Bay to North Head) – including the ocean outfall sites – and data from Sydney Harbour. (2) A distinctive trend of increasing ethane with very significant propane increase includes the coastal data off the entrance to Botany Bay and the vertical profile. Thus, different generic sources of hydrocarbons can be characterised by their distinctive molecular compositions in coastal seawater samples.

The equipment on *Rig Seismic* can detect parts per billion concentrations of light hydrocarbons in seawater. The data from this pilot survey demonstrate that the equipment is very sensitive in both detecting and tracing the dispersion of light hydrocarbon plumes. Furthermore, the composition of the plumes may be used to identify generic sources of the hydrocarbons.

This continuous profiling capability aboard *Rig Seismic* is a unique tool with potentially wide application. For example, analytical instruments can be fitted to the tow-fish for continuous profiling of other parameters, such as dissolved oxygen fluorescence and turbidity in seawater, while, simultaneously, volatile compounds can be determined by instruments linked to the gas flow extracted from the seawater. This gas can be collected for subsequent shore-based isotopic analyses. Other dissolved (but non-volatile) compounds, such as seawater nutrients (nitrogen, phosphate and silicon), dissolved organic carbon, and heavy metals, can be analysed at sea, in the flowing seawater stream, or samples may be collected for later shore-based analysis.

Furthermore, continuous geochemical tracer (CGT) data can be obtained on *Rig Seismic* simultaneously with remotely sensed high-resolution seismic reflection, side-scan sonar and bathymetric data. These integrated data-collection systems have a wide range of applications in marine geoscience, including exploration for offshore resources and environmental monitoring.

Fig. 31. A – Concentrations of total volatile hydrocarbons (THC) and methane in the coastal transect survey from Botany Bay to North Head. B – Concentrations of ethane, propane and butane in the coastal transect survey from Botany Bay to North Head.

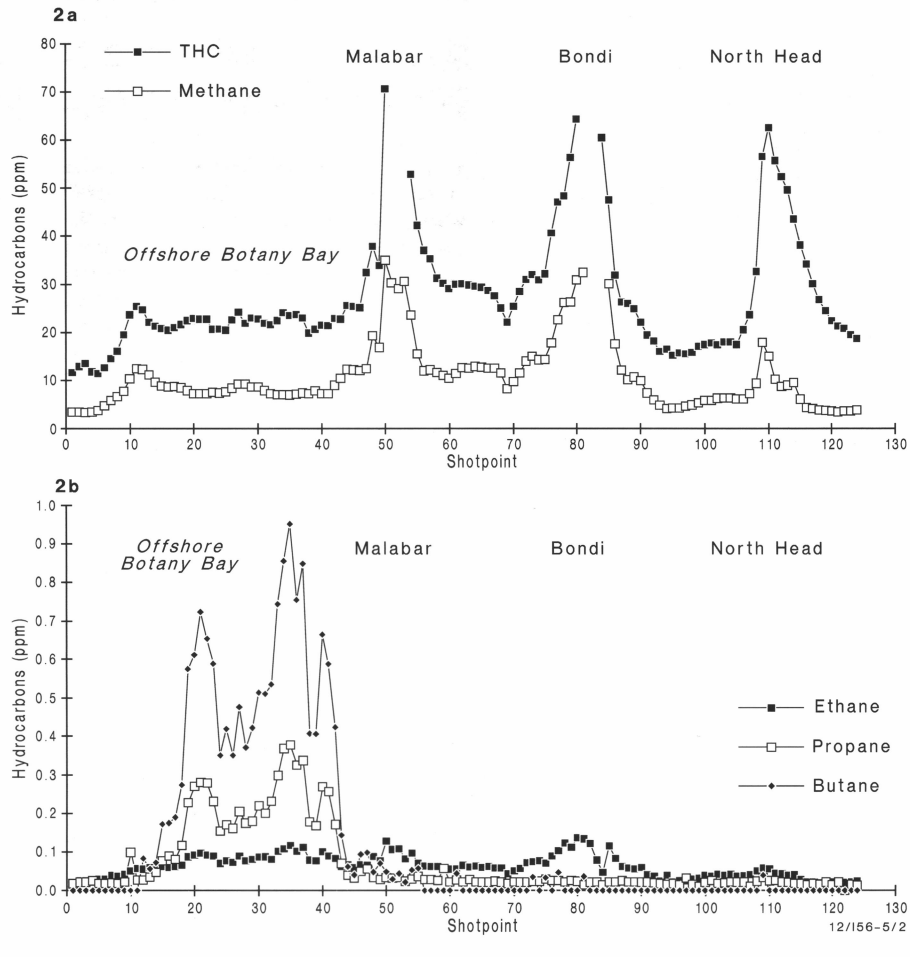

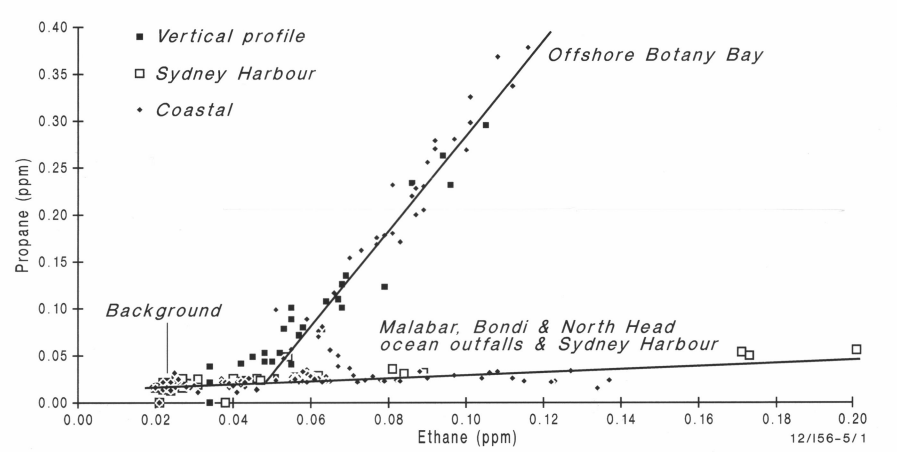

Fig 32. Cross-plot of ethane vs. propane for all data collected during the survey.

For further information contact Dr David Heggie, Mr Gary Bickford or Mr Jeremy Bishop at BMR (Marine Geosciences and Petroleum Geology Program).

BMR GEOLOGY AND GEOPHYSICS AUSTRALIA

The BMR Research Newsletter is published twice a year, in April and October. For further information please contact BMR Marketing & Information Section, tel. (06) 249 9623, fax 257 6466. Correspondence relating to the BMR Research Newsletter should be addressed to The Editor, BMR Research Newsletter, Bureau of Mineral Resources, GPO Box 378, Canberra ACT 2601, tel. (06) 249 9111, fax (06) 247 2728.

 ISSN 0813-751 X.

B92/21419 Cat. No. 92 2018 3. Printed by Pirie Printers Pty Limited, PO Box 438, Fyshwick ACT 2609.